

**Palacký University in Olomouc  
Faculty of Science  
Department of Geology**



**Controlling factors of porosity formation in sandstone; the case study in the Karpatian  
sediments, Carpathian Foredeep, Czech Republic**

**Bachelor thesis**

**Peshawa Alshahi**

**Petroleum Engineering program  
Full time study  
Supervisor: Mgr. Daniel Šimíček, Ph.D.**

**Olomouc 2024**

## **Controlling factors of porosity formation in sandstone; the case study in the Karpatian sediments, Carpathian Foredeep, Czech Republic**

### **Anotace**

Studované území se nachází ve střední části moravského regionu (východní Čechy) a zahrnuje izolované výchozy karpatských sedimentů, které jsou významnými ložisky ropy a zemního plynu. Terénní práce probíhaly na dvou lokalitách: Símře a Dolní Nětčice. Na Símře byl pro terénní měření použit gamaspektrometr spolu s podrobnými makroskopickými popisy a fotodokumentací. V Dolních Nětčicích byl výchoz odebrán pro optickou mikroskopickou analýzu. Hlavním cílem této práce je popsat geologické faktory ovlivňující pórovitost karpatských pískovců. Studie byla provedena na vzorcích karpatských (spodní miocenních) sedimentárních hornin ze dvou výchozů. Úsek Símře je souvislý výchoz o tloušťce 570 cm, v Dolních Nětčicích jsou nesouvislé výchozy podél soutěsky potoka. Na obou lokalitách byly provedeny litologické popisy, odběry vzorků a měření gama spektrometrem. Na Símře bylo provedeno 20 gama spektrometrických měření od 0 cm do 475 cm pomocí GT-32 super spec s 25 cm intervaly mezi měřeními. Čtyři vzorky sedimentárních hornin ze Símře a tři z Dolních Nětčic byly připraveny jako tenké řezy pro optickou analýzu. Komplexní analýza těchto vzorků odhalila zásadní poznatky o souhře mezi původem, diagenetickými faktory a výslednou pórovitostí a propustností pískovců. Vyšší pórovitost a propustnost jsou spojeny s lepším tříděním, méně zaoblenými tvary zrn a méně rozsáhlou cementací a změnami jílu, zatímco nižší pórovitost a propustnost souvisí se špatným tříděním, subangulárními tvary zrn a významnou přítomností cementování a jílu. Měření gama spektrometrie (GRS) ukazují, že vyšší hodnoty GRS, odrážející vyšší obsah jílu a těžkých minerálů, odpovídají nižší porozitě. Vrstvy štěrku s vysokou porézností vykazují nízké hodnoty K, U a Th, zatímco prachovitý jíl s nízkou porozitou vyazuje vyšší hodnoty GRS. Protokol Standard Gamma-Ray (SGR) poskytuje komplexní pohled na přirozené gama záření, koreluje vyšší radioaktivní obsah s nižší porozitou a naopak.

### Annotation

The study area is situated in the central part of the Moravian region (eastern Czech Republic) and includes isolated outcrops of Karpatian sediments, which are significant oil and natural gas reservoirs. Fieldwork was conducted at two localities: Símře and Dolní Nětčice. At Símře, a gamma spectrometer was used for field measurements, along with detailed macroscopic descriptions and photo documentation. At Dolní Nětčice, the outcrop was sampled for optical microscopic analysis. The main aim of this thesis is to describe the geological factors influencing the porosity of Karpatian sandstones. The study was conducted on samples of Karpatian (Lower Miocene) sedimentary rocks from two outcrops. The Símře section is a continuous outcrop 570 cm thick, while Dolní Nětčice features discontinuous outcrops along a stream gorge. Lithological descriptions, sampling, and gamma-ray spectrometer measurements were performed at both sites. At Símře, 20 gamma-ray spectrometric measurements were taken from 0 cm to 475 cm using the GT-32 super spec, with 25 cm intervals between measurements. Four sedimentary rock samples from Símře and three from Dolní Nětčice were prepared as thin sections for optical analysis. The comprehensive analysis of these samples revealed critical insights into the interplay between provenance, diagenetic factors, and the resulting porosity and permeability of the sandstones. Higher porosity and permeability are associated with better sorting, subrounded grain shapes, and less extensive cementation and clay alteration, whereas lower porosity and permeability are linked to poor sorting, subangular grain shapes, and significant cementation and clay presence. Gamma-ray spectrometry (GRS) measurements indicate that higher GRS values, reflecting higher clay and heavy mineral content, correspond to lower porosity. Gravel layers with high porosity exhibit low K, U, and Th values, while silty clay with low porosity shows higher GRS readings. The Standard Gamma-Ray (SGR) log provides a comprehensive view of natural gamma radiation, correlating higher radioactive content with lower porosity and vice versa.

**Klíčová slova:** Pórovitost, pískovec, Karpatské sedimenty, Símře, Dolní Nětčice.

**Key words:** Porosity, Sandstone, Karpatian sediments, Símře, Dolní Nětčice.

**Number of pages:** 48

**Number of annexes:** 00

I declare that I have prepared the bachelor's thesis myself and that I have stated all the used information resources in the thesis.

In Olomouc, July 22, 2024

Peshawa Alshahi  
.....

## **Acknowledgement**

First and foremost, I wish to thank Allah for providing me with the strength, wisdom, and perseverance necessary to complete this thesis.

I am deeply grateful to my supervisor, Mgr. Daniel Šimíček, for his invaluable guidance, insightful feedback, and unwavering support throughout this research. His expertise and encouragement have been crucial to the success of this work.

I would also like to extend my thanks to my colleagues for their collaboration, assistance, and camaraderie. Your support and insights have greatly contributed to the completion of this project.

To my family, I am profoundly thankful for their constant encouragement, understanding, and patience. Your support has been a pillar of strength throughout this journey.

Thank you all for your invaluable contributions and support.

***Peshawa Alshahi***

**Table of content**

Anotace.....	2
Annotation .....	3
Klíčová slova.....	3
Key words .....	3
Acknowledgement .....	5
List of tables.....	8
List of figures.....	8
1. Introduction.....	10
2. Localization of study area: .....	11
3. Geological Settings.....	12
3.1. Carpathian Foredeep .....	12
3.2. Karpatian depositional cycle.....	14
4. Porosity and Permeability:.....	16
4.1. Types of Porosity: .....	18
4.2 Controlling factors of porosity in sandstone:.....	21
4.2.1. Grain Packing: .....	21
4.2.2 Grain Size: .....	23
4.2.3 Grain Shape:.....	25
4.2.4 Grain Size Distribution: .....	26
5. Methods:.....	27
5.1. Field work: .....	28
5.2 Laboratory work: .....	29
6. Results.....	30
6.1 Lithological description.....	30
6.2 Filed description: .....	32
6.3 Gamma-ray spectrometry .....	34
6.4 Petrographic analysis of thin sections .....	37
7. Discussion .....	41
7.1 Evaluation of provenance and diagenetic factors for the porosity and permeability of sandstones in this case study .....	41

7.2 Evaluation of sensitivity of gamma-ray spectrometry to beds with different porosity.....	44
6. Conclusion.....	46
7. Reference .....	47

### List of tables

**Table 1** Shows the effect of grain shape on porosity. (Ogolo, Naomi & Akinboro, Olorunmbe & Inam, Joseph & Akpokere, Felix & Onyekonwu, 2015)..... 25

**Table 2** Field description of Karpatian sediments at Símře site. .... 33

**Table 3** The concentration of Potassium (K), Uranium (U), Thorium(Th), Th/K ratio, and Standard Gamma-Ray (SGR) in the studied samples of Karpatian sediments at Símře site ..... 35

### List of figures

**Figure 1** Position of the studied localities on a section of the basic map of the Czech Republic. 1 – Símře, 2 - Dolní Nětčice (www1)..... 11

**Figure 2** Simplified geological situation in the eastern part of the Czech Republic (Moravia region) (www2)..... 12

**Figure 3** Geological situation in the vicinity of studied localities (www3);1- Símře site, 2- Dolní Nětčice site..... 13

**Figure 4** Stratigraphic division of the Karpatian stage in the southern and northern parts of the Carpathian Foredeep (Brzobohatý et al., 2003)..... 15

**Figure 5** Cubic packing (a), rhombohedral (b), cubic packing with two grain sizes (c), and typical sand with irregular grain shape (d). (Ahmed K. Alshara, 2020)..... 17

**Figure 6** Relationships of Porosity vs Permeability cross plot with statsmodel prediction. (Andy McDonald, 2020)..... 17

**Figure 7** Isolated pores in a compacted bed. (Dr. Sidqi A. Abu-Khamsin, 2004)..... 19

**Figure 8** Shows the Secondary porosity by solution..... 19

**Figure 9** Shows the Secondary porosity by dolomitization of calcite..... 20

**Figure 10** Shows the Secondary porosity by fractures. (Dr.Jawad.Alassal, Yahya Jirjees, Ali, Mohamedali, Shaho, Sajad, Sara, Namiq, Mohammed, 2017)..... 20

**Figure 11** Shows the Ordered packing arrangements of spherical grains and resulting maximum porosity (in percentage). (Bandara, K.M.A.S., Ranjith, P.G. & Rathnaweera, 2019) ..... 21

**Figure 12** Shows the cubic packing of identical spheres, (Glover, P., 2001)..... 22

**Figure 13** Grain size classification of siliciclastic sediments. (Wentworth, 1922). .... 24

**Figure 14** Shows the relation between porosity, grain size and grain shape. (Glover, P., 2001) . 24

**Figure 15** Apparent volume for assemblages of spheres of different diameter ratios. (Glover, P., 2001) ..... 26

**Figure 16** The Símře site ..... 28



**Figure 17** Lithological column of Karpatian sediments at Símře site with the marked sampling position for thin sections. .... 31

**Figure 18** Vertical variation of Potassium (K), Uranium (U), Thorium(Th), Th/K ratio, and Standard Gamma-Ray (SGR) within studied beds of Karpatian sediments at Símře site. .... 36

**Figure 19** (S1) thin section of Simre site shows Quartz (QZ), Dolomite clay matrix (Dol. C.M.), Clay matrix (C.M.), Feldspar (FLDS), Plagioclase dissolution (P. Dis.) and Rock fragment (R. FR). .... 37

**Figure 20** (DN1) thin section of Dolní Nětčice site shows Quartz (QZ), Dolomite clay matrix (Dol. C.M.), Clay matrix (C.M.), Feldspar (FLDS), Plagioclase dissolution (P. Dis.) and Rock fragment (R. FR). .... 38

**Figure 21** (DN2) thin section of Dolní Nětčice site shows Quartz (QZ), Dolomite clay matrix (Dol. C.M.), Clay matrix (C.M.), Fossils and Rock fragment (R. FR). .... 39

**Figure 22** (DN3) thin section of Dolní Nětčice site shows Quartz (QZ), Clay matrix (C.M.), Fossil, Plagioclase dissolution (P. Dis.), Dissolution surface (Dis. Surface) and Rock fragment (R. FR). .... 40

**Figure 23** Calculation of porosity for (S1) sample from Simre site by using imagej software. .. 42

**Figure 24** Calculation of porosity for (DN1) sample from Dolní Nětčice site by using imagej software. .... 43

**Figure 25** Calculation of porosity for (DN2) sample from Dolní Nětčice site by using imagej software. .... 43

**Figure 26** Calculation of porosity for (DN3) sample from Dolní Nětčice site by using imagej software. .... 44

## **1. Introduction**

The study area is situated in central part of Moravian region (the eastern part of the Czech republic). There are isolated outcrops of the Karpatian sediments, which are an important collector rocks of oil and natural gas in the Czech Republic. The porosity and permeability of sedimentary rocks are essential factors in determining their geotechnical qualities. They are especially important for determining the suitability of a certain rock as a natural hydrocarbon reservoir. The research part of the thesis focuses on the description of the geological setting in the vicinity of studied localities, with special attention to the sediments of the Karpatian age. There is also a Section describing types of porosity and geological factors that contribute to the resulting porosity of siliciclastic sedimentary rocks. In the field phase, two localities with outcrops of the Karpatian sedimentary rocks were visited. At the Símře site, a field measurement was carried out with a gamma spectrometer, which is the outcrop equivalent of the gamma-ray well-logging method. A detailed macroscopic description and photo documentation of the sedimentary succession was also carried out here. In the Dolní Nětčice site, in addition to the macroscopic description, the outcrop was sampled for optical microscopic analysis. The laboratory phase of the thesis includes the stage analysis of thin sections using optical microscopy. The shape and roundness of the grains, grain size, grain packing and modal composition of sandstones were determined in thin sections. Photos of thin sections were subjected to image analysis in order to calculate the apparent porosity volume in samples. The main aim of this thesis is to describe the main geological factors that contribute to the resulting porosity of the studied sandstones.

## 2. Localization of study area:

The case study was carried out on samples of the Karpatian (Lower Miocene) sedimentary rocks. The beds of these rocks represent collectors for natural gas in central and northern Moravian regions of the Czech Republic. Most of the Karpatian sedimentary rocks are currently buried under younger sedimentary rock of the Carpathian Foredeep or flysch nappes of the Outer Western Carpathians. Only outcrops of the Karpatian sedimentary rocks are situated in Central Moravia, on an area roughly defined between the towns of Přerov in the east, Lipník nad Bečvou in the north and Bystřice pod Hostýnem in the south. Two outcrops of the Karpatian sediments were studied here (Fig. 1). The first locality is called Símře which is 35 km south-eastern far from Olomouc City and 12 km south-east far from Hranice city. The inactive sandpit is situated eastern of defunct settlement of Símře (GPS: 49°27'40.355"N, 17°37'46.806"E; cadastral territory of Soběchleby village). The second locality is called Dolní Nětčice is located on the northeastern edge of the cadastral territory of Dolní Nětčice village (GPS: 49°29'28.019"N, 17°40'49.342"E) (Fig 1). These are small, intermittent outcrops of individual layers in the gorge of an unnamed stream.



**Figure 1** Position of the studied localities on a section of the basic map of the Czech Republic. 1 – Símře, 2 - Dolní Nětčice (www1).

### 3. Geological Settings

#### 3.1. Carpathian Foredeep

Studied area is located close to the boundary of two basic geological units in the Czech Republic which are Bohemian Massif and the Outer Western Carpathians. The Outer Western Carpathians are represented on our territory by molasse sediments of the Carpathians foreland and flysch sediments of the Western Carpathians (Fig. 2), which were thrust onto the autochthonous foreland in the form of nappes.

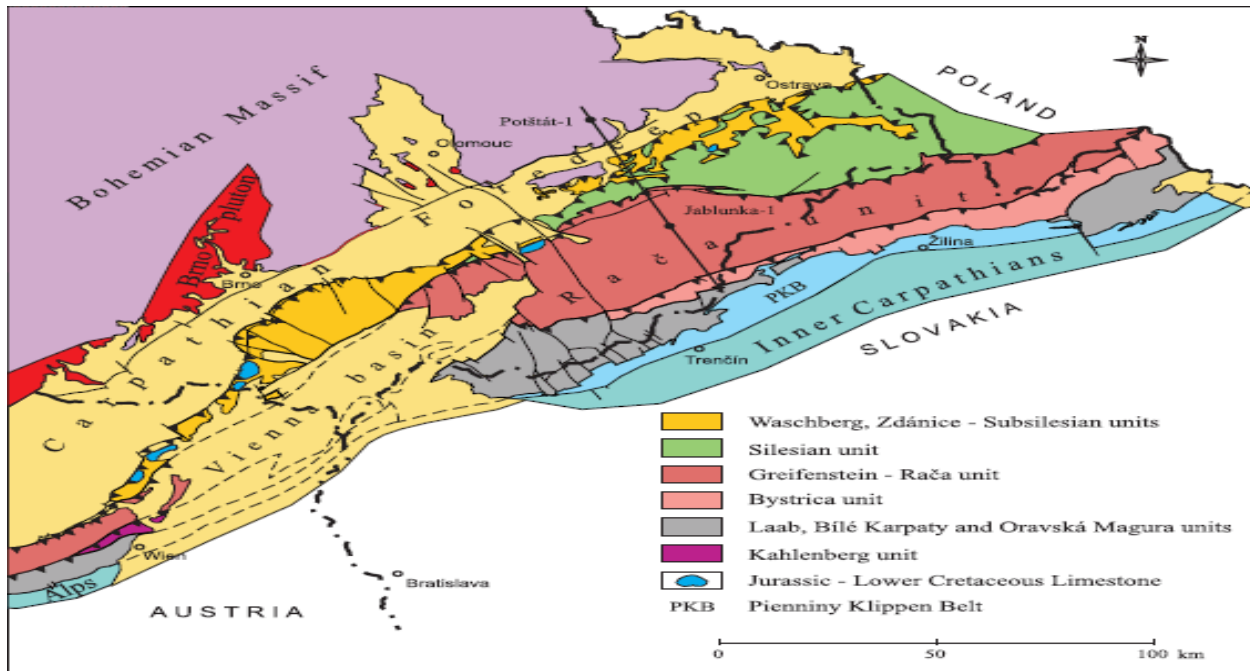


**Figure 2** Simplified geological situation in the eastern part of the Czech Republic (Moravia region) (www2).

The Carpathian foreland also known as the Carpathian Foredeep is a large geological and geographical region in Europe which can be found in the Czech Republic, Poland, Ukraine and Romania. The Czech part of the Carpathian Foredeep evolved during the Neogene period. It was originated by several reasons which include collision of tectonic plates, subsidence, sedimentation, climate and environmental factors (Sanders et al., 2002). The Czech part of the Carpathian Foredeep is a system of sub-basins with the Bohemian Massif bedrock, which are filled with marine molasse sediments (Eggenburgian–Badenian). The subsidence axis of sub-basins receded on the Bohemian Massif foreland before the advancing flysch accretionary wedge. The syn-depositional thrusting of the flysch nappes caused that the sediments of the

foredeep are partially buried under the flysch nappes or are even incorporated into the nappes (Fig. 3). According to numerous boreholes, the total thickness of the Carpathian Foredeep in Moravia is in the order of hundreds of meters, only locally it can exceed 1000m (Kostelníček, Petr, Vladimír Ciprys, and Jirů Berka, 2006)

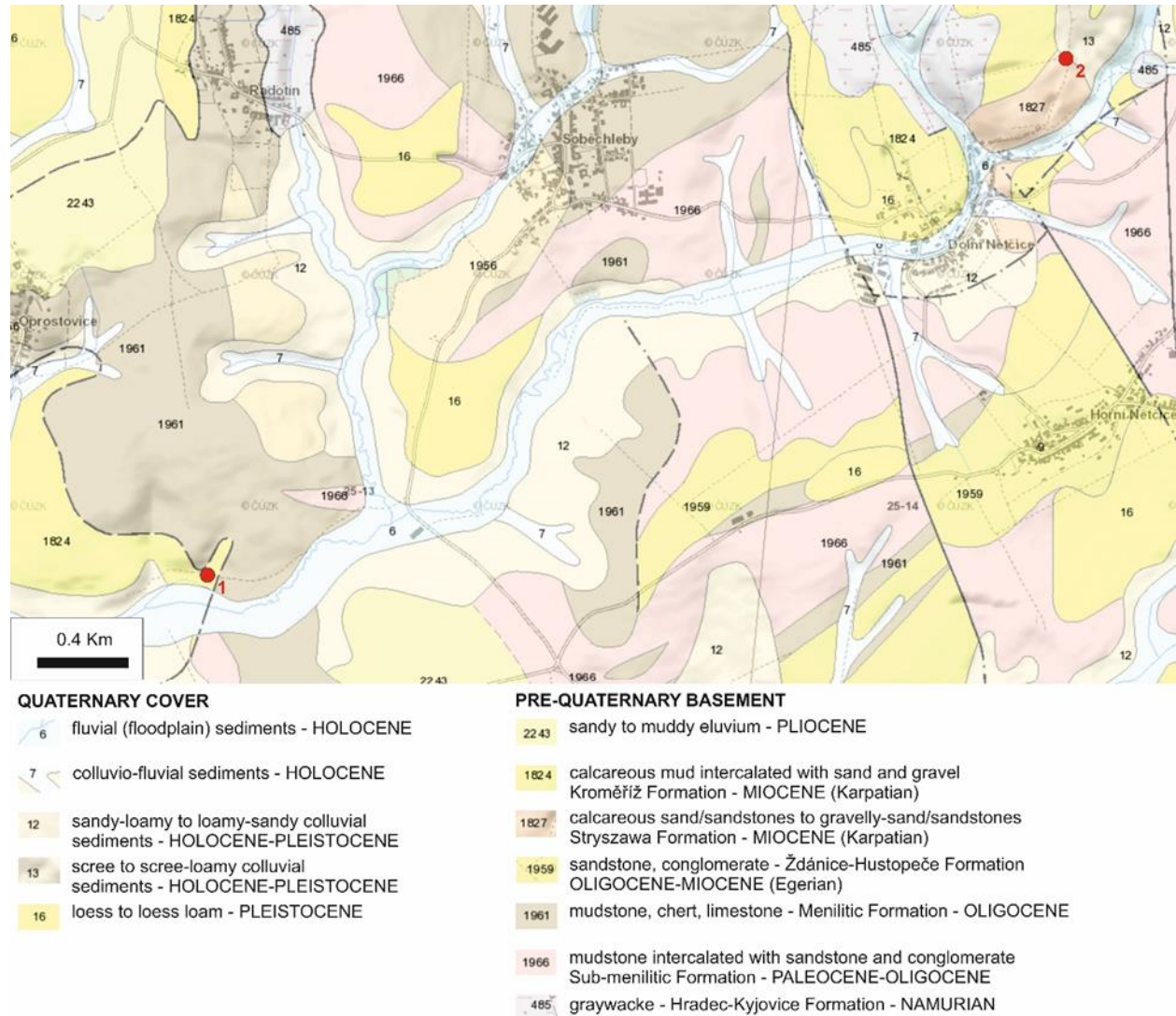


**Figure 3** Geological situation in the vicinity of studied localities (www3); 1- Símře site, 2- Dolní Nětčice site.

The Neogene Carpathian Foredeep in Moravia originated as one of the depositional subsystems within the Paratethys region. From the point of view of Paratethian stratigraphy, three main depositional units can be distinguished: 1. Eggenburgian–Ottangian, 2. Karpatian and 3. Badenian. Each of these units is characterized by a specific depositional regime, which is the result of tectonic processes within the Carpathians orogenic belt and global sea level changes.

Due to the focus of the research, the work exclusively describes the Karpatian stage of the development of the Carpathian Foredeep in Moravia. Based on the different structure and stratigraphic extent of the basin-fill, the Carpathian Foredeep is divided into three main parts: Southern, Central and Northern Foredeep. The study area is situated close to the tectonic line that represents the northern limit of the Upper Morava Basin and also forms the border between the northern and central parts of the Carpathian Foredeep. (Golonka, Jan, and Frank J. Picha, 2006)

### **3.2. Karpatian depositional cycle**

The geological setting of the Karpatian sediments in the Czech Republic reflects a complex interplay of tectonics, global sea level changes, and sedimentary processes, resulting in a variety of sedimentary facies and depositional environments preserved in the rock record. The age of the rocks in Karpatian stage is characterized from approximately 17.5 to 16.4 million years ago (Brzobohatý et al., 2003). The stratigraphy of the Karpatian Stage in the Czech Republic is characterized by sedimentary sequences deposited in various environments during this time period. In the Czech Republic, the Karpatian Stage is often divided into several formations or members based on lithological characteristics, fossil content and stratigraphic relationships. The onset of the Karpatian sedimentation cycle is associated with strong tectonic activity and thrusting of the flysch accretionary wedge to the NW on the Bohemian Massif foreland. The folding of the nappes of the Pouzdřany and Ždánice Units took place and the Carpathian Foredeep acquired present-day NE-SW direction during the Karpatian stage. Intensive subsidence occurred mainly in southern and central part of the foredeep. In the southern part of the Carpathian foredeep, the Laa Formation was deposited. It is stratigraphically equivalent to the Kroměříž Formation in the central part and the Stryzawa Formation in the northern part of the Carpathian Foredeep (Fig. 4; Brzobohatý et al., 2003). Towards the end of the Karpatian stage, the foredeep became a narrow and shallow basin extending along the front of the Carpathian fold-thrust belt.

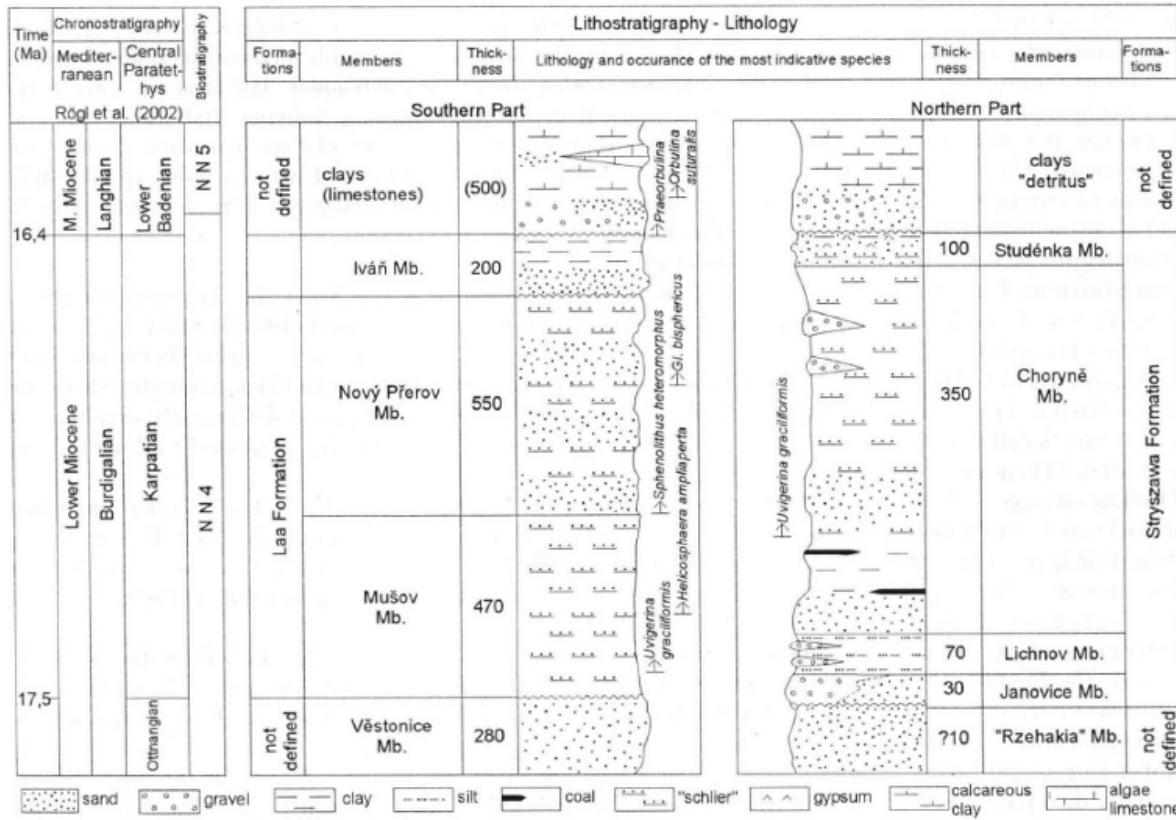


**Figure 4** Stratigraphic division of the Karpatian stage in the southern and northern parts of the Carpathian Foredeep (Brzobohatý et al., 2003).

Sediments of the Kromčříž Formation were studied at the Símře locality (Francírek et al., 2016). The Kromčříž Formation represents the youngest sediments of the Karpatian stage in the central part of the Carpathian Foredeep. Stratigraphically, it overlies the Nový Přerov Member, The youngest member of the Laa Formation in the southern part of the Carpathian Foredeep. The formation is divided in two facies: “Holešov Conglomerate” and “Variegated Beds”. The Holešov Conglomerate consists of gravel and sand. The gravels consist mainly of quartz, dark chert, sandstone, silicified limestone, Upper Jurassic limestone and quartzite clasts. Pebbles of metamorphic rocks, granite and mudstone are rare. The source area was the Ždánice-Hustopeče Formation of the Ždánice-Subsilesian Unit. The facies of Holešov Conglomerate is present at the Símře locality (Bubík et al., 2017). The typical facies of the Variegated Beds are "pebbly mudstones", ie., the sediments formed by an admixture of sandy and gravelly fractions in a muddy matrix resulting from deposition from the gravity density currents. The Variegated Beds are documented only from the boreholes. The source area was the Silesian unit.

The Dolní Nětčice locality belongs to the Stryzawa Formation. As a result of tectonics, the sediments of the Stryzawa Formation were deposited in a basin with a highly rugged relief, which corresponds to the considerable facies diversity of the formation. The Janovice, Lichnov, Choryně and Studénka Members are defined within the Stryzawa Formation. The Janovice Member (formerly “the basal Karpatian clastics”) is represented by weakly consolidated arkose sandstones and conglomerates, non-calcareous fine-grained sandstones with glauconite, rarely with intercalations of grey marlstone. The thickness of the member reaches up to 36 m. The Janovice Member is referred to as the Dolní Nětčice Member (the locality is the subject of my study) in the central Moravia. The Dolní Nětčice Member is represented by grey, yellowish-grey, fine- to medium-grained calcareous sandstone intercalated with marlstones and conglomerates. The Lichnov Member of the Stryzawa Formation (formerly “Variegated Beds”) is represented by bluish, greenish-grey, rusty, and reddish-brown siltstones to sandy siltstones. They reach a thickness of up to 70 m. The Choryně Member of the Stryzawa Formation (formerly “the Brown and Grey Member”) contains mainly brown, brown-grey to green-grey mudstone, which gradually pass into whitish-grey, fine- to coarse-grained sandstones with coal seams and horizons rich in plant detritus and brackish molluscs. The thickness of the Choryně Member decreases to the NE. The Studénka Member of the Stryzawa Formation (formerly “Variegated Beds with gypsum”) is formed by a finely rhythmic alternation of variegated calcareous mudstone with siltstone and fine-grained calcareous sandstone. There are places with gypsum and pelosiderite in places.

#### **4.Porosity and Permeability:**

Porosity is defined as the fraction of the bulk rock volume  $V$  that is not occupied by solid matter.

If the volume of solids is denoted by  $V_s$ , and pore volume as  $V_p = V - V_s$  we can write the porosity

as:

$$\emptyset = \frac{V - V_s}{V} = \frac{V_p}{V} = \frac{PORE\ VOLUME}{TOTAL\ BULK\ VOLUME}$$

(Abhijit Y. Dandekar, 2013).

The porosity can be written either as a fraction or as a percentage.

The porosity does not give any information about the size of the pores or their distribution, therefore, rocks of the same porosity can have very different physical properties. For example, a carbonate rock and a sandstone, which might both have a porosity of 0.2, but the carbonate pores



are often very separated, which makes their permeability much lower than that of the sandstone, (Abhijit Y. Dandekar,2013).

Based on its origin, porosity can be divided into primary and secondary porosity. Primary porosity is created during the deposition of sediments. Secondary porosity is caused by various post-depositional geological processes (see Section 4.2) with a contribution of factors such as soil stress, vadose and groundwater circulation, etc. Fractures or the formation of solution voids often increase the original porosity of the rock. (K.L. Milliken, 2003).

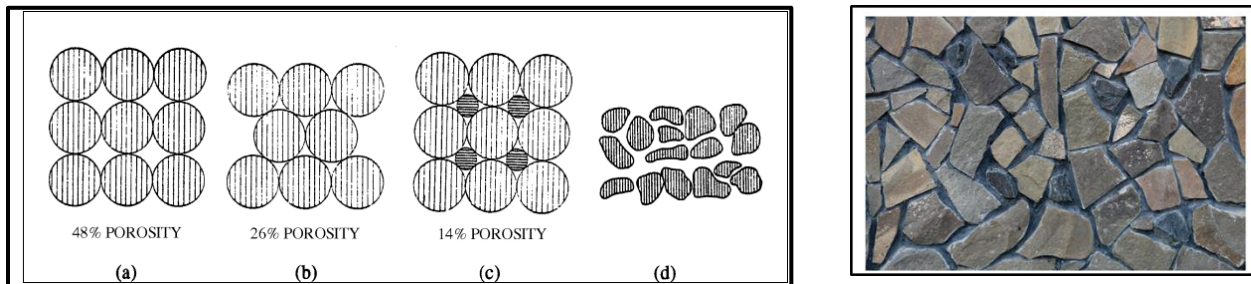


**Figure 5** Cubic packing (a), rhombohedral (b), cubic packing with two grain sizes (c), and typical sand with irregular grain shape (d). (Ahmed K. Alshara, 2020).

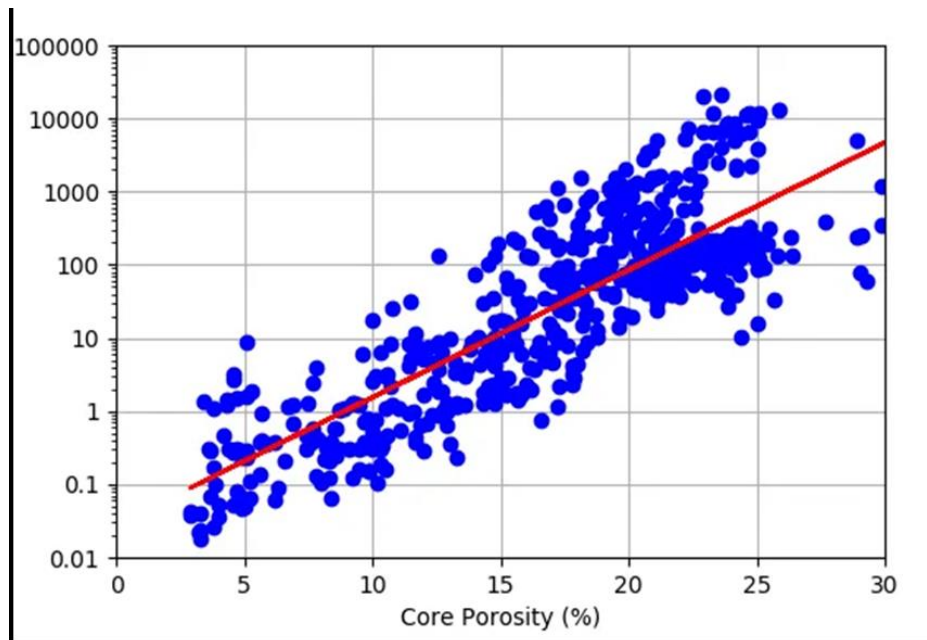


**Figure 6** Relationships of Porosity vs Permeability cross plot with statsmodel prediction. (Andy McDonald, 2020).

For a uniform rock grain size, porosity is independent of the size of the grains. A maximum theoretical porosity of 48% is achieved with cubic packing of spherical grains, as shown in (Fig. 5a.) Rhombohedral packing, which is more representative of reservoir conditions, is shown in (Fig. 5b;) the porosity for this packing is 26%, If a second, smaller size of spherical grains is introduced into cubic packing (Fig. 5.c), the porosity decreases from 48% to 14%. Thus, porosity is dependent on the grain size distribution and the arrangement of the grains, as well as the amount of cementing materials. Not all grains are spherical, and grain shape also influences porosity. A typical reservoir sand is illustrated in (Fig. 5.d.) (Andy McDonald, 2020).

Permeability in the context of oil and gas refers to the ability of the reservoir rock to allow the flow of fluids such as oil, natural gas, and water through its pore spaces. It is a crucial parameter in petroleum engineering and geology as it directly impacts the productivity and recovery of hydrocarbons from subsurface reservoirs. Permeability is a key component of reservoir characterization, alongside porosity and fluid saturation. Together, these properties help determine the storage capacity, fluid flow behavior, and overall producibility of a reservoir. Permeability is typically measured in units of darcies (D) or millidarcies (mD), with 1 D being equivalent to a flow rate of 1 cubic centimeter per second under a pressure gradient of 1 atmosphere per centimeter. Reservoir permeability can range from extremely low values in tight formations (e.g., shale) to very high values in highly permeable sandstone or carbonate reservoirs. (Aldoury, Muzher, 2010).

### **4.1. Types of Porosity:**

Because of the variety and complexity of sedimentation processes, several types of porosity can be formed such as (primary porosity, secondary porosity, fracture porosity, vuggy porosity, effective (open) porosity, ineffective (closed) porosity, dual porosity). There is also a division of pores according to size (macroporosity, mesoporosity, microporosity). Then there is also the morphological classification of porosity (intergranular, intragranular, shelter, fenestral, mouldic, intercrystalline). Usually, the porosity that arises after initial sedimentation is simple. All grains

are loosely packed and pores within the sediments are connected. Fluids can migrate through-and fill the entire pore space. Invariably, however, post-depositional processes alter the pore space

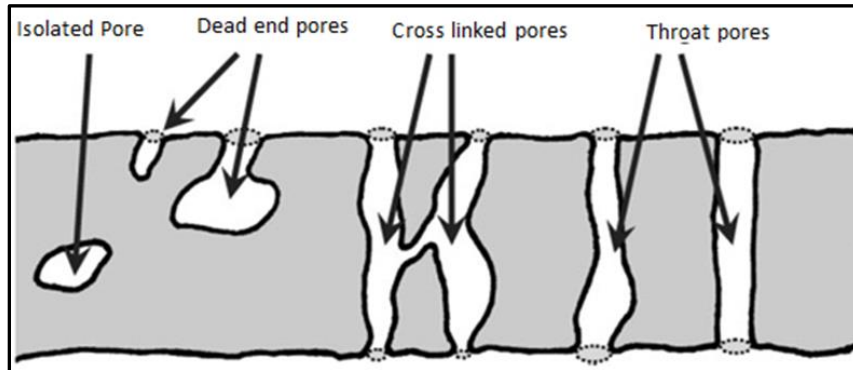


**Figure 7** Isolated pores in a compacted bed. (Dr. Sidqi A. Abu-Khamsin, 2004)

by several ways. As the weight of the sediments increase, compaction presses grains closer to each other causing some pores to be closed and isolated from the rest of the pore space (Fig. 7). Although compaction reduces the pore volume a little, more importantly, it makes some of the pore space inaccessible to fluid flow. Therefore, part of the fluids within the reservoir cannot be produced as it is trapped within the isolated pores.

The effective porosity is defined, hence, as the fraction of the bulk volume of a sample that is connected pore space. (Sidqi A. Abu-Khamsin, 2004).

Reduction of pore volume and isolation of pores can also be a result of secondary deposition. Brines that flow through the rock could deposit minerals of various types between the grains, usually at the grain-to-grain contacts. Such deposits cement grains together, but could also plug pore throats or even fill entire pores. In other instances, brine can dissolve some of the grain material causing pore enlargement, which creates extra porosity (Fig.8). For this reason, the initial porosity is referred to as the primary, intergranular\_ or matrix porosity while the porosity, modified

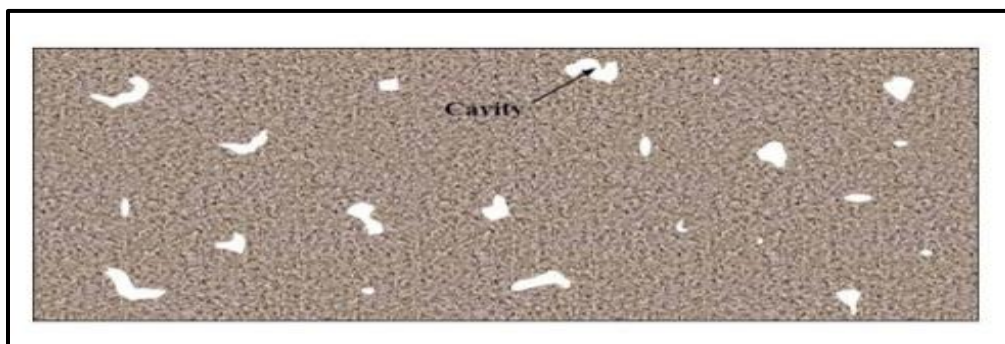


**Figure 8** Shows the Secondary porosity by solution.

by various post-depositional processes, is referred to as the secondary one Porosity, (Aloki Bakhtiari et al., 2011). Secondary porosity can also be created by cation exchange between the water and the rock. For example, some of the calcium ions in

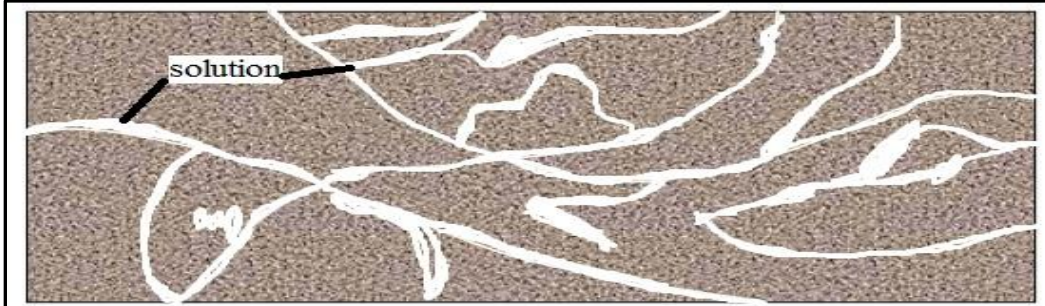


**Figure 9** Shows the Secondary porosity by dolomitization of calcite.

calcite crystal may be replaced by magnesium ions from the brine, which forms the mineral dolomite  $\text{CaMg}(\text{CO}_3)_2$ . Since dolomite has a smaller molar volume than calcite, this causes shrinkage of the grains and, thus, secondary porosity (Fig.9). Fractures created within the rock also contribute to secondary porosity as see in (Fig.10).

Diagenesis plays a considerable role in controlling the quality of a reservoir within a trap. Solution can enhance reservoir quality by generating secondary porosity, whereas cementation can destroy it. In some situations, diagenesis can generate a hydrocarbon trap (Rittenhouse, 1972). Oil or gas moving up a permeable carrier bed may reach a cemented zone, which inhibits further migration.

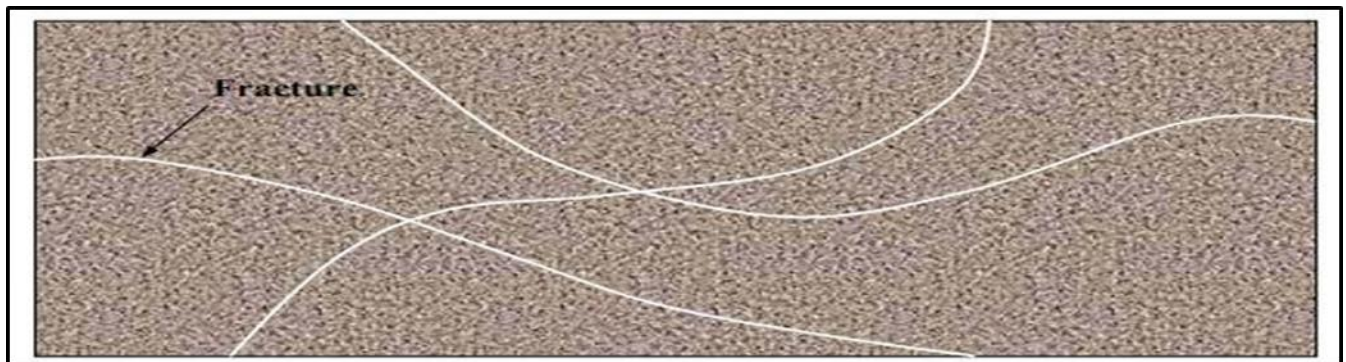


**Figure 10** Shows the Secondary porosity by fractures. (Dr.Jawad.Alassal, Yahya Jirjees, Ali, Mohamedali, Shaho, Sajad, Sara, Namiq, Mohammed, 2017).

**4.2 Controlling factors of porosity in sandstone:**

The initial (pre-diagenetic) porosity is affected by three major structural parameters these are grain size, grain packing, particle shape, and the distribution of grain sizes. (William W. Woessner, Eileen P. Poeter, 2020) The mentioned parameters are determined by the geological situation in the source area. They reflect character of transport and the conditions at the place of deposition. The mineral composition of sedimentary material can also have an influence on porosity, because some minerals are chemically less stable, subject to alteration, which during diagenesis affects the cementation and authigenesis of minerals. Both of these diagenetic processes affect porosity and permeability. However, the initial porosity is rarely that found in real rocks as these have subsequently been affected by secondary controls on porosity such as compaction and geochemical diagenetic processes. This section briefly reviews these controls. The interchange of chemicals at the sediment/water column contact, frequently with the aid of microbes, is part of the early diagenetic phase. The final stages of diagenesis are associated with the sediment burial, and the function of lithification processes (compaction, pressure dissolution, cementation, authigenesis) is critical. (Peter Santschi, Patrick Höhener, Gaboury Benoit, Marilyn Buchholtz-ten Brink,1990).

**4.2.1. Grain Packing:**

Grain packing, also known as particle packing or granular packing, refers to the arrangement and distribution of individual solid particles within a bulk material or medium. It is a fundamental concept in scientific fields, including Geology and Petroleum engineering. It is possible to

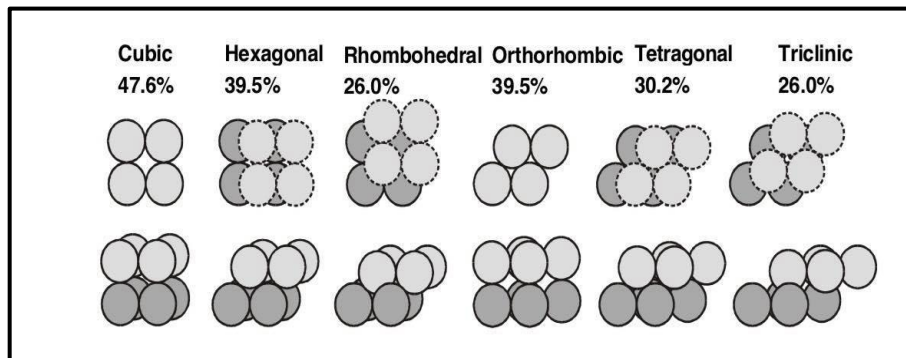


**Figure 11** Shows the Ordered packing arrangements of spherical grains and resulting maximum porosity (in percentage). (Bandara, K.M.A.S., Ranjith, P.G. & Rathnaweera, 2019)

compute the theoretical porosities for different grain packing patterns. (Robert L. Folk, 1980). Also, the important geological factor that influences on grain packing is sedimentation and transportation. (Fig.11) shows theoretical maximum porosity for a cubic packed rock made up of uniformly sized spherical grains is 47.6%, and it is independent of grain size.

The bulk volume of the cell  $V_{\text{bulk}} = L^3$ , and the number of spheres in the cell  $n = (L/2r)^3$ . Hence the volume of the matrix  $V_{\text{matrix}} = (4n r^3)/3 = (L/2r)^3 (4n r^3)/3 = (n L^3)/6$ . The porosity can now be calculated from Eq. (2) as:

$$\phi = \frac{L^3 - (\pi L^3 / 6)}{L^3} = (1 - \pi / 6) = 0.4764$$

(Glover, P., 2001)

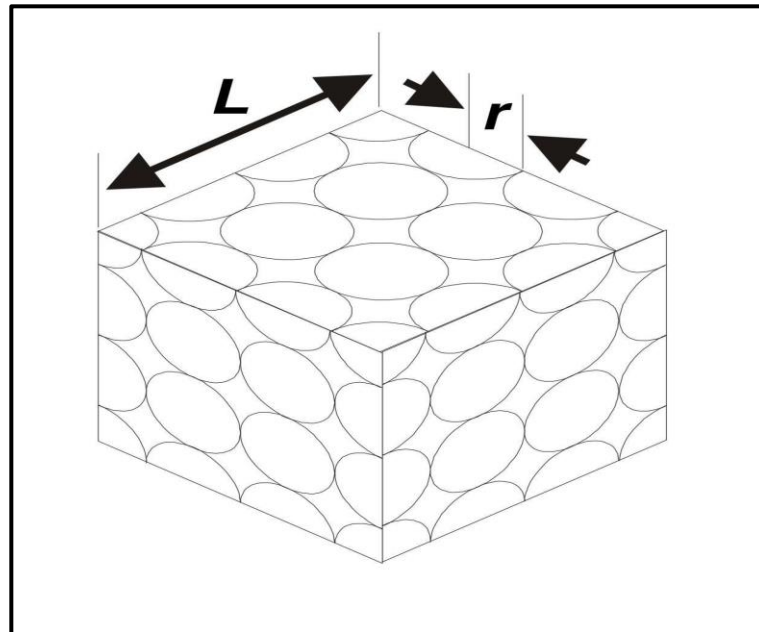


**Figure 12** Shows the cubic packing of identical spheres, (Glover, P., 2001)

### 4.2.2 Grain Size:

The size of particles is directly dependent on the type of environmental setting, transporting agent, length and time during transport, and depositional conditions, and hence it possesses significant utility as an environmental proxy (McManus, 1988; Stanley-Wood and Lines, 1992). Grain size is related to a multitude of external factors acting on a local or regional scale. For example, in the coastal and marine setting, grain size is related to the bathymetry and geometry of the basin, nutrient regime, biogeochemical oceanography, coastal processes, sedimentary inputs from land sources, and outputs. As mentioned before, the ordered cubic packing of identical spheres leads to grain size independent porosity. This is also true for the other ordered packing lattices, but not for the random spherical configuration. Ordered packings do not occur in actual depositional settings because they are energetically unstable, and the grains become randomly fragmented. The equilibrium porosity of a porous material formed of a random packing of spherical grains is determined by the rock's stability as a result of frictional and cohesive forces working between individual grains. These forces are proportional to the exposed surface area of the grains. The specific surface area (exposed grain surface area per unit solid volume) is inversely proportional to grain size. When all other conditions are equal, it means that a given weight of coarse grains will be stabilized at a lower porosity than the same weight of finer grains. (Payton, R.L., Chiarella, D. & Kingdon, 2022). (Fig.12), illustrates this basic norm for a sedimentary rock formed of a single grain size. It can be shown that the rise in porosity only becomes substantial at grain sizes smaller than 100,000  $\mu\text{m}$ , and porosities as high as 0.8 have been reported in certain recent sediments. As grain size exceeds 100,000  $\mu\text{m}$ , frictional forces drop and porosity declines until a limit that reflects random frictionless packing is attained, which happens at 0.399 porosity and is independent of grain size is reached. For randomly packed spheres, no additional loss of porosity is conceivable until the grains experience irreversible deformation owing to dissolution recrystallisation, fracture, or plastic flow, and all such losses in porosity are referred to as compaction, as shown in (Fig.13). (E.H. Rutter, C.T. Glover, 2012).

Millimeters (mm)	Micrometers ( $\mu\text{m}$ )	Phi ( $\phi$ )	Wentworth size class	Rock type	
4096		-12.0	Boulder	Conglomerate/ Breccia	
256		-8.0	Cobble		
64		-6.0	Pebble		
4		-2.0	Granule		
2.00		-1.0			
			Very coarse sand	Sandstone	
1.00		0.0	Coarse sand		
1/2	0.50	1.0	Medium sand		
1/4	0.25	2.0	Fine sand		
1/8	0.125	3.0	Very fine sand		
1/16	0.0625	4.0		Siltstone	
1/32	0.0310	5.0	Coarse silt		
1/64	0.0156	6.0	Medium silt		
1/128	0.0078	7.0	Fine silt		
1/256	0.0039	8.0	Very fine silt		
	0.00006	14.0	Clay	Mud	Claystone

Figure 13 Grain size classification of siliciclastic sediments. (Wentworth, 1922).

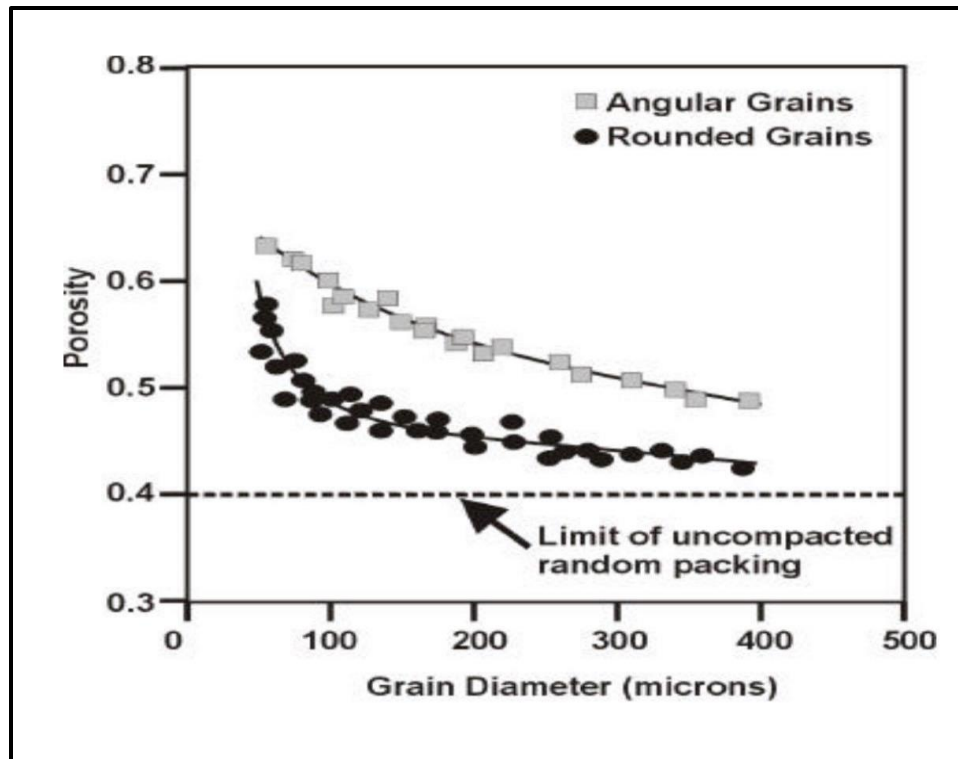


Figure 14 Shows the relation between porosity, grain size and grain shape. (Glover, P., 2001)



#### 4.2.3 Grain Shape:

This parameter is not widely understood. Several studies have been carried out on random packing of none-spherical grains (Zongli Chen, Ying Zhao,2022) , and in all cases the resulting porosities are larger than those for spheres. (see table. 1), and on the other hand, the roundness of grains is primarily influenced by the duration and intensity of transport, as well as the type of transporting agent (e.g., water, wind, ice). During transportation, particles collide with each other and with the surrounding substrate, causing abrasion and wearing down of their edges and corners. Over time, this abrasion results in the rounding of grains. Both shape parameters have an effect on compaction and this also on porosity. (Quanshui Huang, Xing Zhou, Biao Liu, 2023)

**Table 1** Shows the effect of grain shape on porosity. (Ogolo, Naomi & Akinboro, Olorunmbe & Inam, Joseph & Akpokere, Felix & Onyekonwu, 2015).

<b>Grain shape</b>	<b>Maximum porosity (fractional)</b>
Sphere	0.399
Cube	0.425
Cylinder	0.429
Disk	0.453

4.2.4 Grain Size Distribution:

Real rocks have a grain size distribution, and the grain size distribution is frequently multi-modal. The best approach to understand the effect is to consider the variable admixture of grains of two sizes (Fig.15) The porosity of the grain size combination is lowered below that of 100% of each size. Two processes are at work here. Consider a rock with two grain sizes, one of which is one-hundredth the diameter of the other. The first mechanism operates when there are enough bigger grains to form the wide skeleton of the rock matrix. Because the smaller particles may fit into the interstices between the bigger particles, the addition of the smaller particles lowers the porosity of the rock. The second mechanism is as follows; there small grains will have a pore space between them. Clearly, if some volume of these grains are removed and replaced with a single solid larger grain, the porosity will be reduced because both the small grains and their associated porosity have been replaced with solid material. The solid lines GR and RF or RM in (Fig.15) represent the theoretical curves for both processes. Note that as the disparity between the grain sizes increases from 6:3 to 50:5 the actual porosity approaches the theoretical lines. Note also that the position of the minimum porosity is not sensitive to the grain diameter ratio. This minimum occurs at approximately 20 to 30% of the smaller particle diameter. In real rocks we have a continuous spectrum of grain sizes, and these can give rise to a complex scenario, where fractal concepts become useful. (Glover, P., 2001)

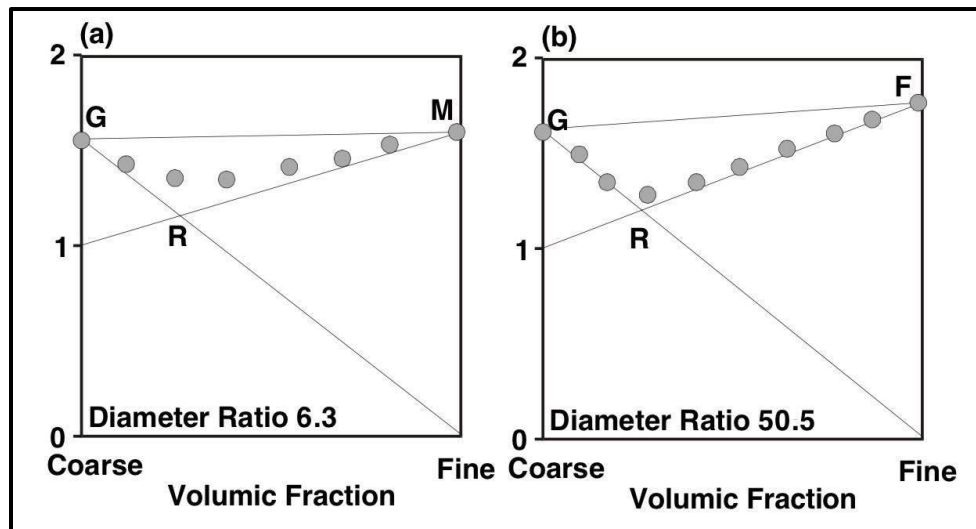


**Figure 15** Apparent volume for assemblages of spheres of different diameter ratios. (Glover, P., 2001)

## 5. Methods:

The work was carried out on two outcrops of Carpathian sediments. The Símře section (GPS: 49°27'40.355"N, 17°37'46.806"E; cadastral territory of Soběchleby village) is a continuous outcrop with a thickness of 570 cm. The Dolní Nětčice site (GPS 49°29'28.019"N, 17°40'49.342"E) represent discontinuous outcrops of individual beds in the gorge of the nameless stream. A lithological description of the rocks, sampling and measurements with a portable gamma-ray spectrometer were carried out at the sites. First it will be outcrop description of macroscopic sedimentary features such as (grain size, sorting, color, thickness). Photo documentation of sight was taken. The Símře site was continuously described from the base upsection. The Dolní Nětčice site was not described in detail due to poor exposure. The description of the rocks was made on the basis of a detailed description of samples taken for optical microscopic analysis. Gamma-ray spectrometry could not even be performed at the site due to the poor exposure of the outcrop. However, gamma-ray spectrometry was performed on Símře site, The levels of potassium (K), uranium (U), and thorium (Th) concentrations were determined using a portable gamma-ray spectrometer called the GT-32 Super Spec. This device is equipped with a 2×2" (103 cm<sup>3</sup>) Bismuth Germanate oxide BGO detector. With a counting duration of 240 seconds for our test, it provides an accuracy of approximately ±10% for assessing K, U, and Th concentrations in sediments with low to moderate radioactivity. (Šimíček & Bábek, 2015).

### 5.1. Field work:

The first site that was studied which was Símře which was 570 cm as mentioned above, that consisted of 12 layers each with different lithological descriptions such as (thicknesses, grain sizes, grain sorting, colors and structures) which will be explained in details in the chapter of results. Also the gamma-ray spectrometric measurements which the was done on the first outcrop 20 times from 0cm to 475 cm by the GT-32 super spec with a time of 240 seconds each time and a distance of 25 cm between measured points. Also four sedimentary rocks were taken as samples from the Símře site and 3 from The Dolní Nětčice site, to prepare thin-sections and analyze them by eyes. The sampling was done from different sandstone facies.



**Figure 16** The Símře site

### **5.2 Laboratory work:**

Petrographic description of thin sections of samples is very useful for determining packing of detrital grains and modal composition of sandstones. grain packing is the theoretical porosities for various grain packing arrangements can be calculated. The thin sections were made by Dr. Jaroslav Kapusta from the UP Department of Geology. They were made from four sandstones (1 from Símře and 3 from Dolní Nětčice). Thin sections were studied by optical microscopy (polarizing microscope Olympus BX50). Thin sections were observed in XPL (cross-polarized light) and PPL (plane-polarized light) mode. Also detrital minerals (e.g., quartz, feldspar, mica), fossils, character of matrix and cement were identified in each thin section. At least 300 grains were identified in each thin section. The thin sections were mounted by blue-colored resin, thanks to which the pores stand out in color. The apparent porosity of the sample was determined in the JMicrovision software for image analysis. The imagej software used for calculating porosity.

## **6. Results**

### **6.1 Lithological description**

The lithological section for Karpatian sediments at the Simre site in the Czech Republic features fine-to-medium grained gravel with poor sorting, subangular clasts, massive stratification, and yellow-gray color with weak consolidation and clay intraclasts at the base. This is followed by a lentil bed of very coarse-grained sand with very poor sorting and floating pebbles, transitioning into fine-grained gravel with cross bedding. Next is fine-to-medium gravel with subangular gravel clasts, massive stratification, and yellow-gray color, weakly consolidated. The gravel gradually transitions to coarse gravel with kaolinized clay galls and CaCO<sub>3</sub> coatings, followed by coarse gravel with floating pebbles and quartz pebbles, showing a decrease in gravel-sized clasts upward. This is succeeded by medium-to-coarse grained sand with floating pebbles, kaolinized layers, and trough cross bedding. Above this are irregular layers of silty clay with ripple lamination, fault disturbances, and kaolinization. The uppermost layers consist of medium-grained, well-sorted sandstone, capped by folded layers of sand and silty clay, showing kaolinization and shard-like breakdown due to solifluction (Fig 17).

# Controlling factors of Porosity in Sandstone Reservoir

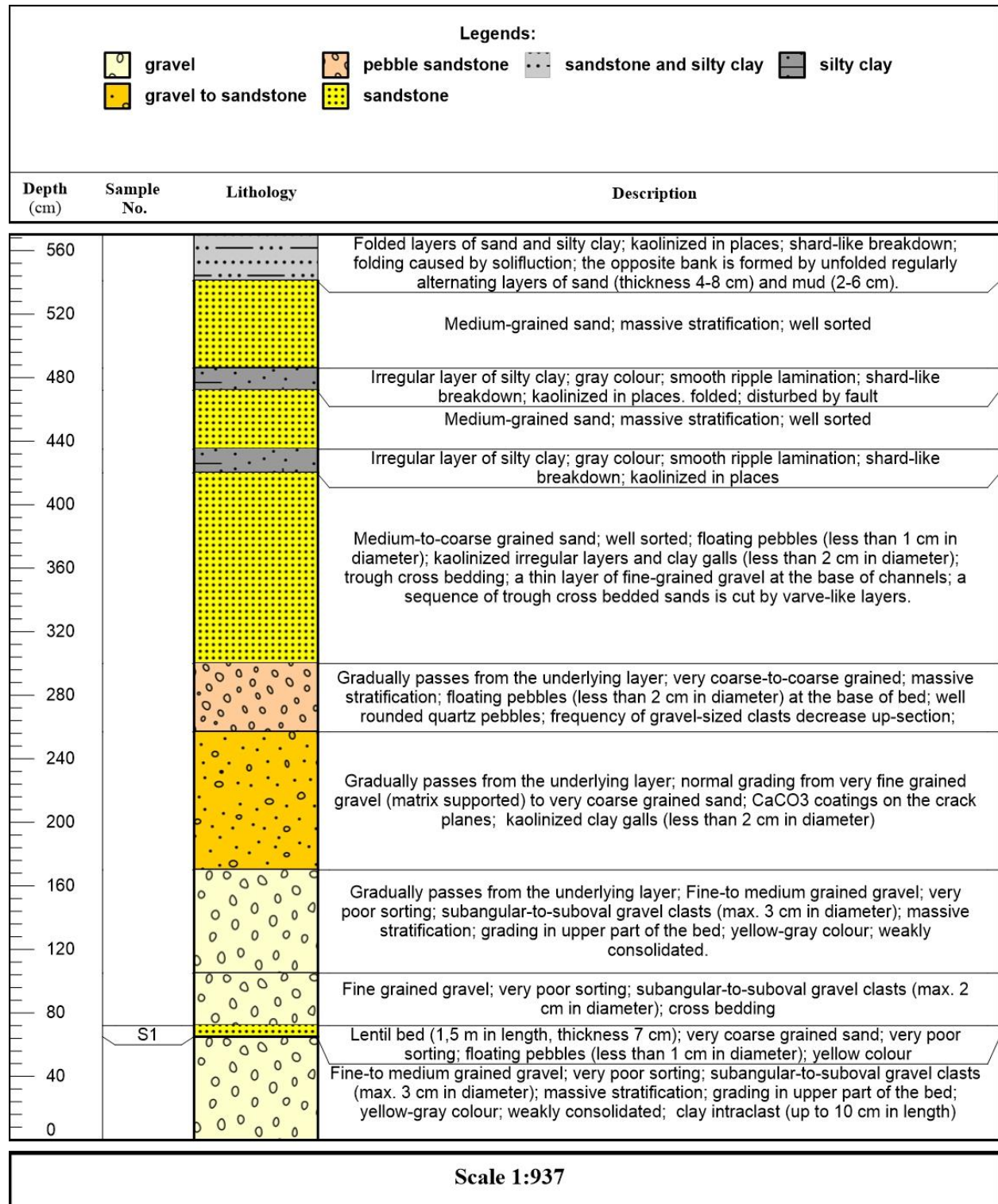


**Figure 17** Lithological column of Karpatian sediments at Simře site with the marked sampling position for thin sections.

## **6.2 Filed description:**

The outcrop at the Simre site in the Czech Republic features a variety of rocks, displaying notable vertical changes in sedimentation. It begins with fine-to-medium grained gravel characterized by very poor sorting, subangular-to-suboval clasts, massive stratification, yellow-gray color, and weak consolidation, along with clay intraclasts. Above this is a lentil bed of very coarse-grained sand, also poorly sorted, with floating pebbles and a yellow hue. Following is fine-grained gravel with similar poor sorting and cross bedding. Gradual transitions are observed into fine-to-medium gravel, which maintains poor sorting but lacks clay intraclasts, and further into very coarse-to-coarse grained sediment with massive stratification, floating pebbles, and quartz pebbles. This transition includes  $\text{CaCO}_3$  coatings and kaolinized clay galls. The sequence continues with medium-to-coarse grained sand, well sorted, containing floating pebbles, kaolinized layers, and trough cross bedding, interspersed with fine-grained gravel at the base of channels and varve-like layers. Higher up, irregular silty clay layers with smooth ripple lamination and kaolinization are found, along with well-sorted, medium-grained sand exhibiting massive stratification. These layers show signs of folding and fault disturbances. The section culminates in folded layers of sand and silty clay, influenced by solifluction, with alternating layers of sand and mud on the opposite bank. Overall, the lithology ranges from gravel and sand to silty clay, with evident vertical changes in sedimentation, including faulting, folding, and varying degrees of sorting and kaolinization, illustrating a complex depositional environment (Table 2).

The Karpatian sediments at the Dolní Nětčice site in the Czech Republic consist of a mix of sedimentary rocks. These include sandstones, varying in grain size from coarse to fine, indicating different depositional environments. Claystones and mudstones are also present, suggesting quieter depositional environments like floodplains or lacustrine conditions. Additionally, conglomerates sporadically occur, suggesting high-energy depositional environments like river channels or alluvial fans. Vertical changes in sedimentation reveal alternating layers of these rock types, reflecting variations in depositional conditions over time.



**Table 2** Field description of Karpatian sediments at Símře site.

Beds	Thickness	Grain size	Sorting	Shape	Color	Structure	Other
Bed 1	65	Fine-to medium grained gravel	Very poor sorting	Subangular to suboval gravel clasts	Yellow–gray	Massive stratification; grading in upper part of the bed	Weakly consolidated, clay intraclast.
Bed 2	7	Very coarse grained sand	Very poor sorting	Floating pebbles	Yellow	-	-
Bed 3	33	Fine grained gravel	Very poor sorting	Subangular to suboval gravel clasts	Yellow	Cross bedding	-
Bed 4	65	Fine-to medium grained gravel	Very poor sorting	Subangular to suboval gravel clasts	Yellow–gray	Massive stratification; grading in upper part of the bed	Weakly consolidated
Bed 5	87	Very fine grained gravel to very coarse grained sand	Well sorted	-	Yellow	-	Kaolinized clay galls. CaCO <sub>3</sub> coatings on the crack planes
Bed 6	43	Very coarse to coarse grained	Moderate	Floating pebbles at the base of bed; well-rounded quartz pebbles	Yellow–brown	Massive stratification	Frequency of gravel-sized clasts decrease up-section;
Bed 7	120	Medium to coarse grained sand	Well sorted	Floating pebbles kaolinized irregular layers and clay galls.	Yellow	Trough cross bedding; a thin layer of fine-grained gravel at the base of channels; a sequence of trough cross bedded sands is cut by varve-like layers.	-
Bed 8	15	Silty clay	Moderate	-	Gray	Smooth ripple lamination; shard-like breakdown;	Kaolinized in places
Bed 9	37	Medium-grained sand	Well sorted	-	Gray-brown	Massive stratification	-

Bed 10	14	Silty clay	Moderate	-	Gray	Smooth ripple lamination; shard-like breakdown, folded; disturbed by fault	Kaolinized in places
Bed 11	55	Medium-grained sand	Well sorted	-	Gray-brown	Massive stratification	-
Bed 12	29	Sand and silty clay	Angular	-	Gray-brown	Folded layers, folding caused by solifluction. the opposite bank is formed by unfolded regularly alternating layers of sand and mud. Shard-like breakdown	Kaolinized in places

### 6.3 Gamma-ray spectrometry

The gamma-ray spectrometry is one of the most important well-logging techniques used in the petroleum industry for the evaluation of lithological parameters in the wells. The intensity of the gamma radiation emitted by the rock and received by the scintillation detector quickly decreases with the increasing distance from the detector due to the absorption of photons by the rock matter (Daniel et.al., 2011). The concentration of Potassium (K), Uranium (U) and Thorium (Th) in addition to Th/K ratio and Standard Gamma-Ray (SGR) determined by using the Gamma Ray spectrometry for the Símře site (Table 2).

The K content in the studied samples ranges from 1.6% to 2.5% with an average (1.86 %), the U content range from 1ppm to 3 ppm with an average (1.66ppm) and the Th content range from 4.1ppm to 12.4ppm with an average (6.16 ppm).

The Th/K ratio also calculated; its concentration varies from 2.157 to 5.217 with an average (3.259).

In addition to these, the equation of Rider (1999) used to calculate Standard Gamma-Ray (SGR) for studied samples. The results show that its concentration range from 52.326 to 113.802 (67.993 avg.)

$$SGR = U * 8.09 + Th * 3.93 + K * 16.32 \quad (\text{Rider, 1999})$$

In general, as we notice the concentration of K, U, Th, Th/U and SGR increase as we go upward from the oldest layers to youngest layers, however there are some negative deflections as well specially at depth 325cm (Fig. 10).

**Table 3** The concentration of Potassium (K), Uranium (U), Thorium(Th), Th/K ratio, and Standard Gamma-Ray (SGR) in the studied samples of Karpatian sediments at Símře site

Depth (cm)	DR	K (%)	U (ppm)	Th (ppm)	Th/K	SGR (API)
0	43.2	1.9	1.5	4.1	2.157895	59.256
25	44.2	1.9	1.1	4.9	2.578947	59.164
50	43.8	1.9	1.2	4.4	2.315789	58.008
75	44.9	1.9	1.3	4.8	2.526316	60.389
100	39.2	1.7	1.1	4.1	2.411765	52.756
125	39.5	1.6	1.2	4.2	2.625	52.326
150	44.3	1.7	1.4	5.5	3.235294	60.685
175	44	1.9	1	4.9	2.578947	58.355
200	45.7	1.9	1.4	4.8	2.526316	61.198
225	44.6	1.7	1.6	5.4	3.176471	61.91
250	42.8	1.7	1.4	4.8	2.823529	57.934
275	52.9	1.7	2.1	6.8	4	71.457
300	48.9	1.8	1.7	6.1	3.388889	67.102
325	42.5	1.9	1.1	4.5	2.368421	57.592
350	50.1	1.8	2.3	5.4	3	69.205
375	50.7	1.6	2.4	6.3	3.9375	70.287
400	60.4	1.9	2	9.2	4.842105	83.344
425	58.9	1.9	2.1	8.6	4.526316	81.795
450	75.6	2.3	2.3	12	5.217391	103.303
475	82.2	2.5	3	12.4	4.96	113.802

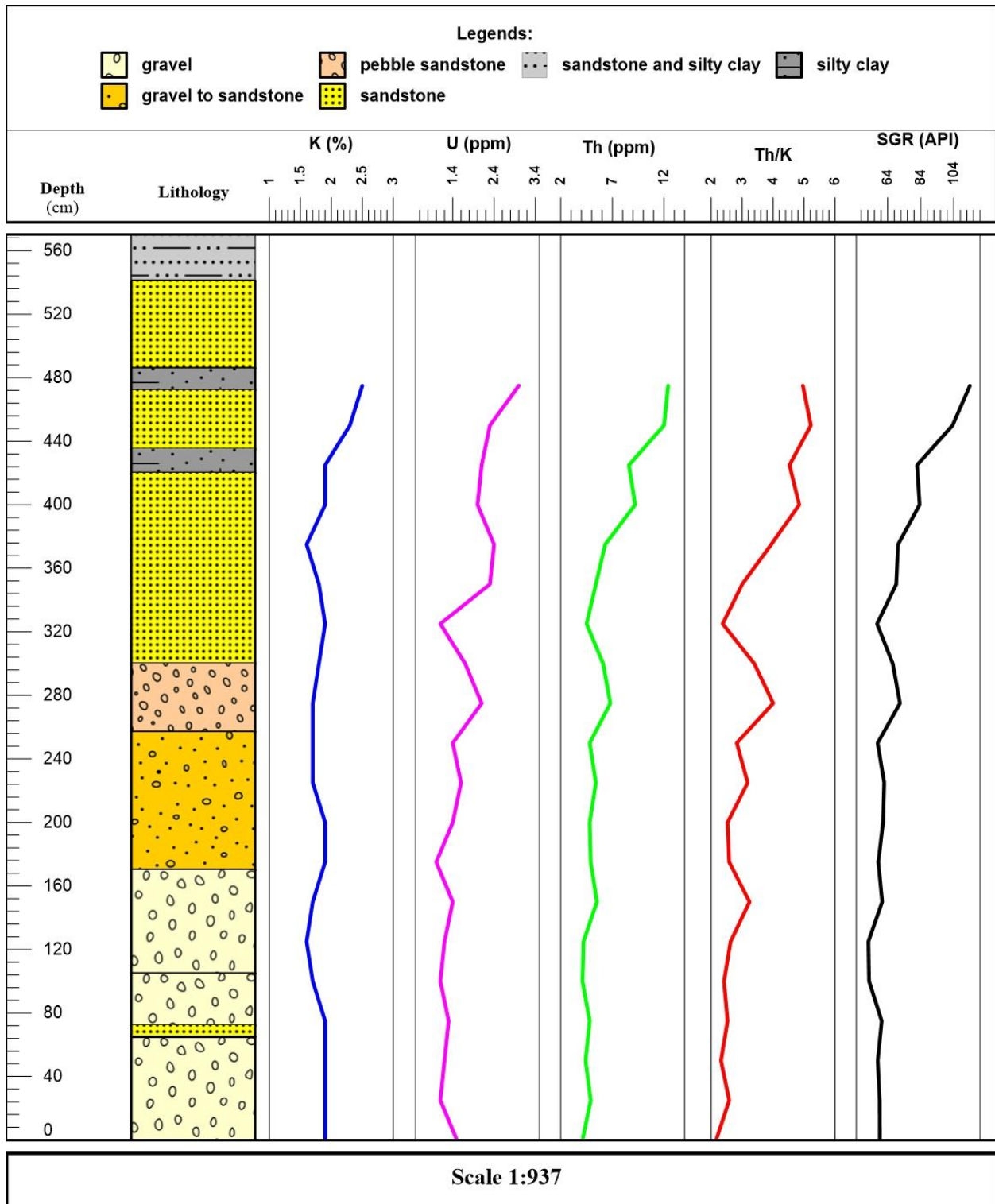


**Figure 18** Vertical variation of Potassium (K), Uranium (U), Thorium (Th), Th/K ratio, and Standard Gamma-Ray (SGR) within studied beds of Karpatian sediments at Símře site.

#### 6.4 Petrographic analysis of thin sections

Thin sections have been prepared for four samples: one from the Simre site (S1) and three from the Dolní Nětčice site (DN1, DN2, and DN3).

Grains Shapes of (S1) are mostly subrounded, with moderate sphericity. Grain Packing are loosely packed, with significant pore space and primarily point contacts. Quartz is abundant and dominant, accompanied by feldspar. Rock fragments are visible in some sections. The matrix is clay-rich. Cementation includes both calcite and dolomite types, with dolomite being notable. Grains are moderately sorted based on the variability in grain sizes, with a significant amount of matrix material. Diagenetic Features includes presence of calcite cement and some clay alteration around feldspar grains (Fig. 19).

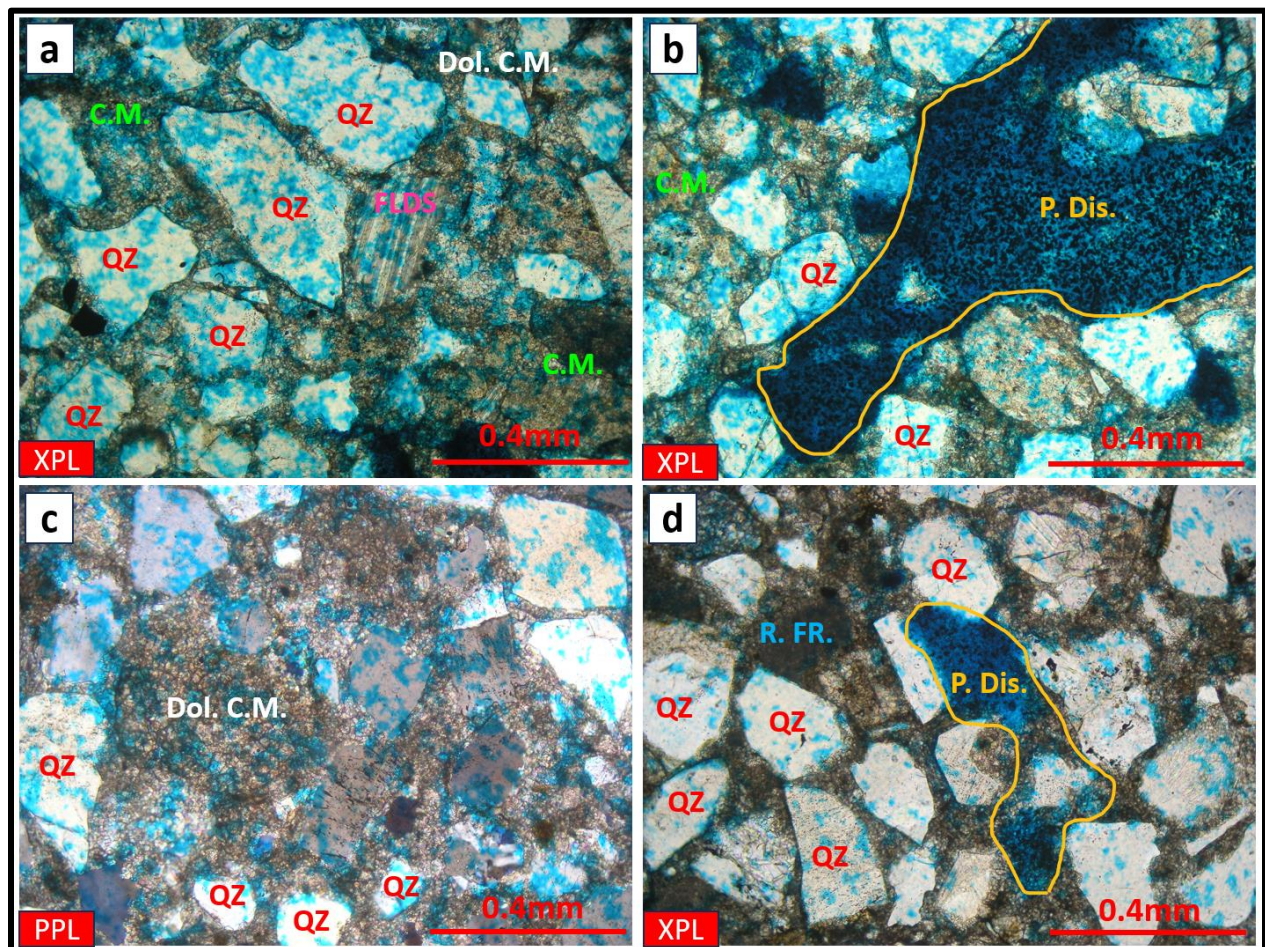


**Figure 19** (S1) thin section of Simre site shows Quartz (QZ), Dolomite clay matrix (Dol. C.M.), Clay matrix (C.M.), Feldspar (FLDS), Plagioclase dissolution (P. Dis.) and Rock fragment (R. FR.).

The (DN1) grains shapes are mostly subangular, with moderate sphericity. Quartz is abundant and dominant, accompanied by feldspar. Rock fragments are visible in some sections. The matrix is clay-rich. Cementation includes both calcite and dolomite types, with dolomite being notable. Grains are poorly sorted based on the variability in grain sizes, with a significant amount of matrix material. Diagenetic Features includes presence of calcite cement and some clay alteration around feldspar grains (Fig. 20).

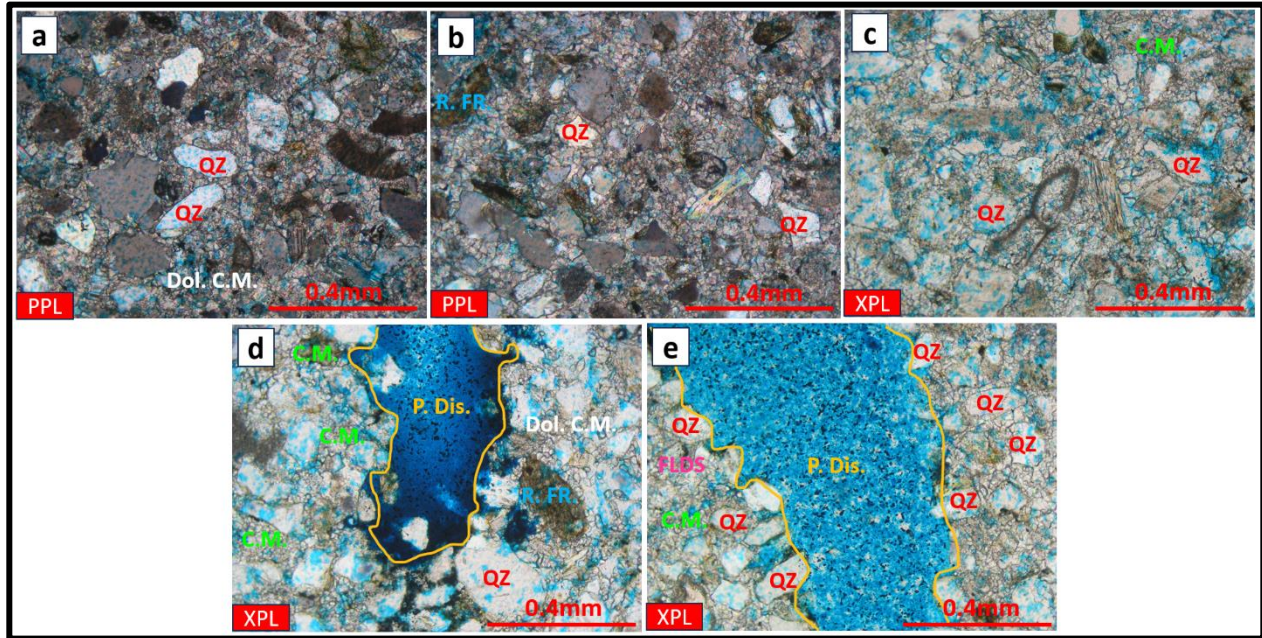


**Figure 20** (DN1) thin section of Dolní Nětčice site shows Quartz (QZ), Dolomite clay matrix (Dol. C.M.), Clay matrix (C.M.), Feldspar (FLDS), Plagioclase dissolution (P. Dis.) and Rock fragment (R. FR).

The (DN2) sample characterized by grains shapes mostly subrounded, with moderate sphericity. Grain Packing are loosely packed, with significant pore space and primarily point contacts. Quartz is abundant and dominant, accompanied by feldspar. Rock fragments are visible in some sections. The matrix is clay-rich. Cementation includes both calcite and dolomite types, with dolomite being notable. Grains are moderately sorted based on the variability in grain sizes, with a significant amount of matrix material. Diagenetic Features includes presence of calcite cement and some clay alteration around feldspar grains (Fig. 21).

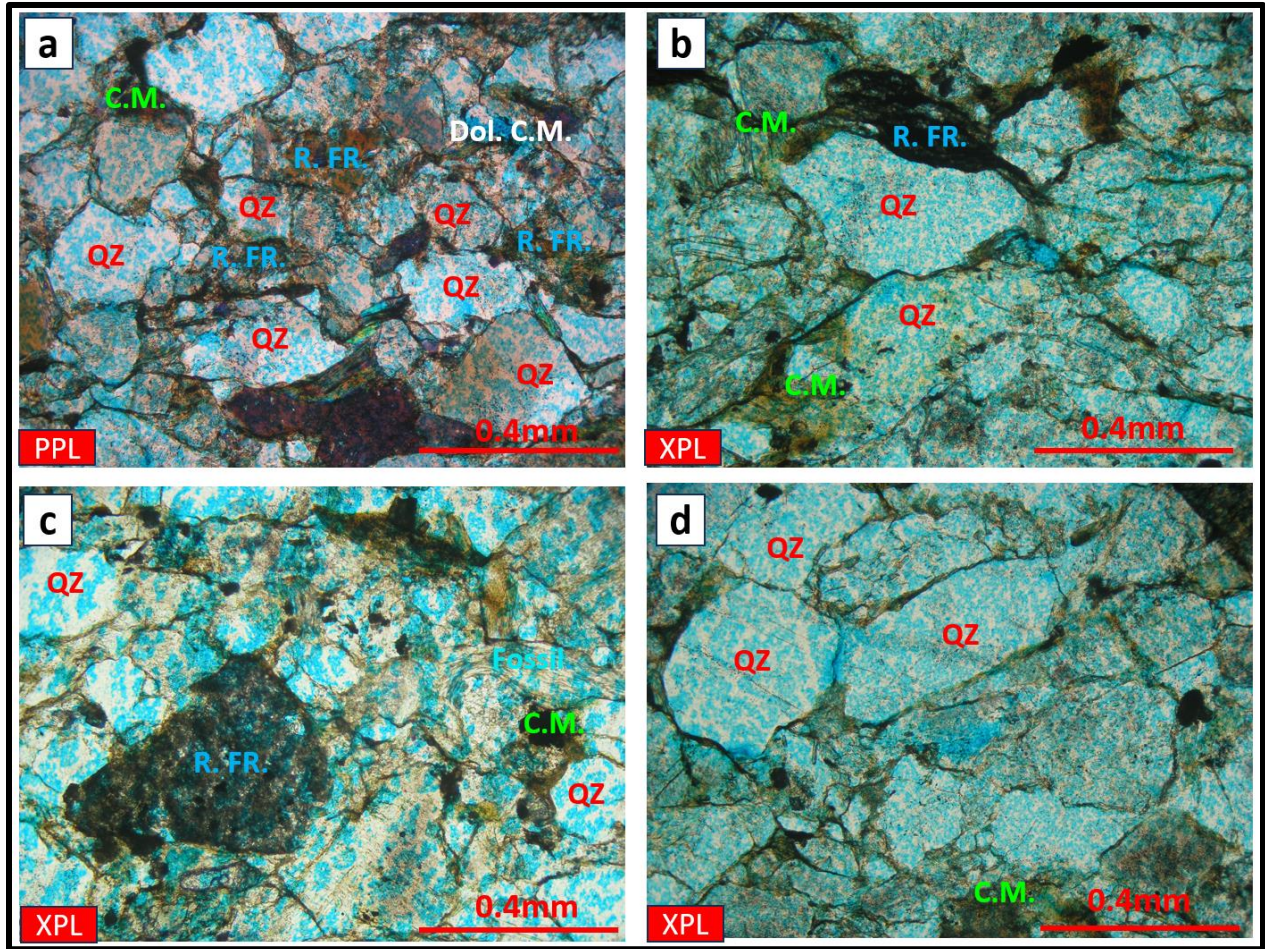


**Figure 21** (DN2) thin section of Dolní Nětčice site shows Quartz (QZ), Dolomite clay matrix (Dol. C.M.), Clay matrix (C.M.), Fossils and Rock fragment (R. FR).

Grain Shape of (DN3) are mostly subangular, with low sphericity. Quartz is abundant and dominant, accompanied by feldspar. Rock fragments are visible in some sections. The matrix is clay-rich. Cementation includes both calcite and dolomite types, with dolomite being notable. Grains are poorly sorted based on the variability in grain sizes, with a significant amount of matrix material. Diagenetic Features includes presence of calcite cement and some clay alteration around feldspar grains (Fig. 22).

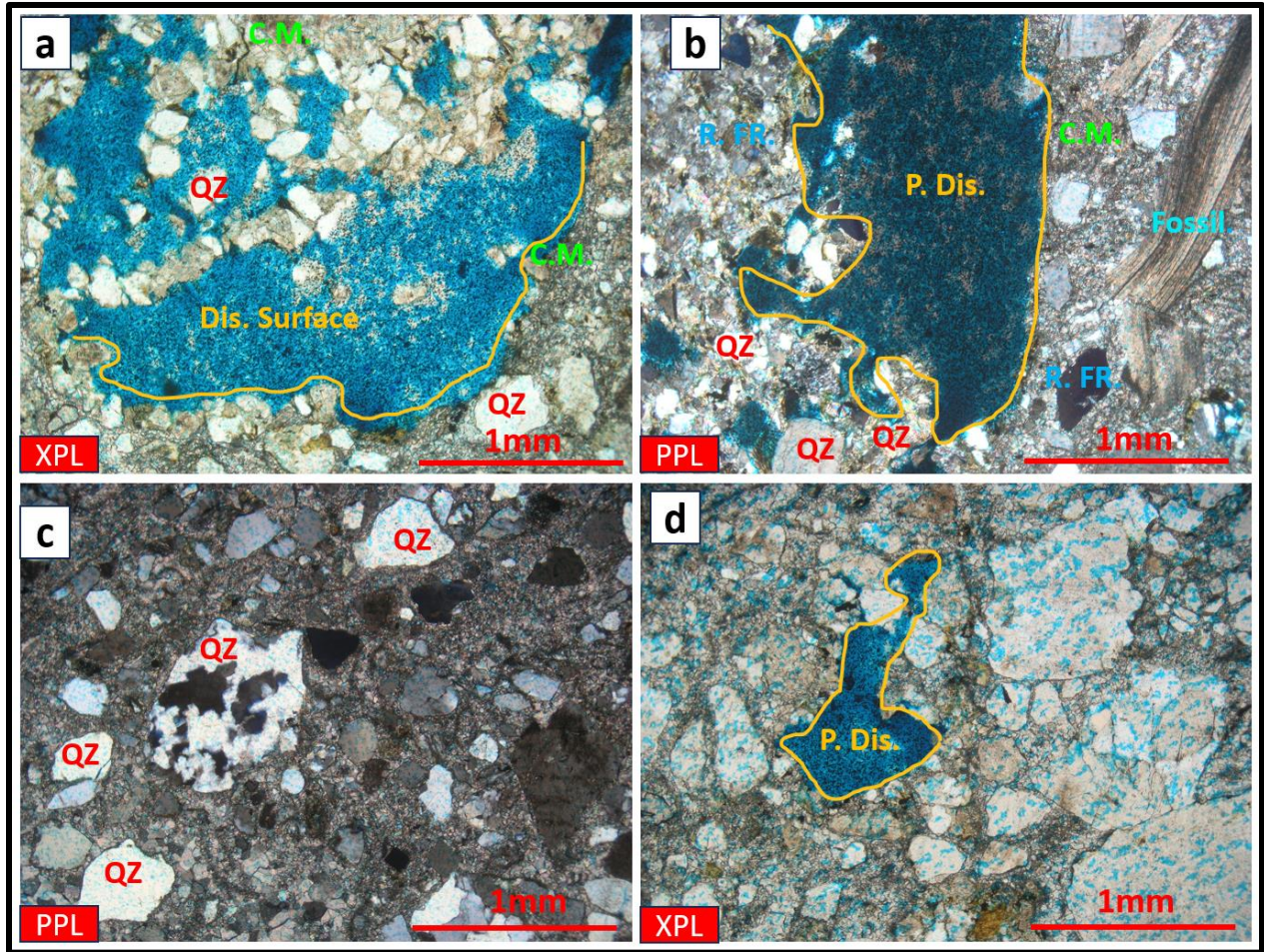


**Figure 22** (DN3) thin section of Dolní Nětčice site shows Quartz (QZ), Clay matrix (C.M.), Fossil, Plagioclase dissolution (P. Dis.), Dissolution surface (Dis. Surface) and Rock fragment (R. FR).



## 7. Discussion

### 7.1 Evaluation of provenance and diagenetic factors for the porosity and permeability of sandstones in this case study

In this study, we evaluated the provenance and diagenetic factors affecting the porosity and permeability of sandstone samples from two distinct sites: Simre (S1) and Dolní Nětčice (DN1, DN2, DN3). The primary focus was on the relationship between porosity and permeability with grain size, sorting, shape, and other intrinsic properties of the sandstone. The analysis of these samples provides insight into how these factors interplay to influence reservoir quality.

The grain size and sorting of the sandstone samples play a critical role in determining porosity and permeability. Well-sorted sandstones generally have higher porosity and permeability because the uniform grain size allows for more efficient packing and larger pore spaces. Conversely, poorly sorted sandstones tend to have lower porosity and permeability due to the presence of fine-grained materials that fill the pore spaces, obstructing fluid flow. The S1 sample is moderately sorted with significant variability in grain sizes, which contributes to its porosity of 12.32%. The moderate sorting allows for a relatively high porosity by maintaining adequate pore spaces, though the presence of matrix material slightly reduces overall permeability. DN1 and DN3 are poorly sorted, resulting in lower porosities of 10.02% and 9.41%, respectively. The poor sorting in these samples reduces permeability due to the heterogeneity in grain sizes that disrupts pore continuity. DN2, on the other hand, is moderately sorted like S1, with a porosity of 12.23%, indicating better porosity and likely better permeability compared to DN1 and DN3.

Grain shape and sphericity significantly influence the packing of grains and thus the porosity and permeability. Subrounded grains tend to pack more loosely than subangular grains, resulting in higher porosity and permeability. The grains are mostly subrounded with moderate sphericity, contributing to a looser packing structure and significant pore space. This morphology is conducive to higher porosity and permeability. Both samples have subangular grains, which pack more tightly than subrounded grains, reducing pore space and thereby porosity and permeability. DN1 and DN3 show lower porosities of 10.02% and 9.41%, respectively. Similar to S1, DN2 has subrounded grains with moderate sphericity, contributing to its higher porosity of 12.23%.

The type and extent of cementation have a profound impact on the porosity and permeability of sandstones. Calcite and dolomite cements are prevalent in all samples, and the presence of these minerals can significantly reduce porosity by filling pore spaces. Both samples exhibit calcite and dolomite cementation but maintain higher porosity (12.32% and 12.23%, respectively). This suggests that while cementation is present, it has not completely occluded the pore spaces, possibly due to the initially better sorting and grain packing. These samples show similar types of cementation but have lower porosities (10.02% and 9.41%, respectively). The poorer sorting and subangular grain shapes likely contribute to a more effective occlusion of pore spaces by cementation.

The clay-rich matrix and diagenetic alterations, such as clay around feldspar grains, also affect porosity and permeability. Clays can occupy pore spaces and swell upon contact with fluids, further reducing permeability. The clay-rich matrix is a common feature, contributing to reduced permeability across the board. The presence of clay alteration around feldspar grains, as noted in all samples, likely exacerbates this effect.

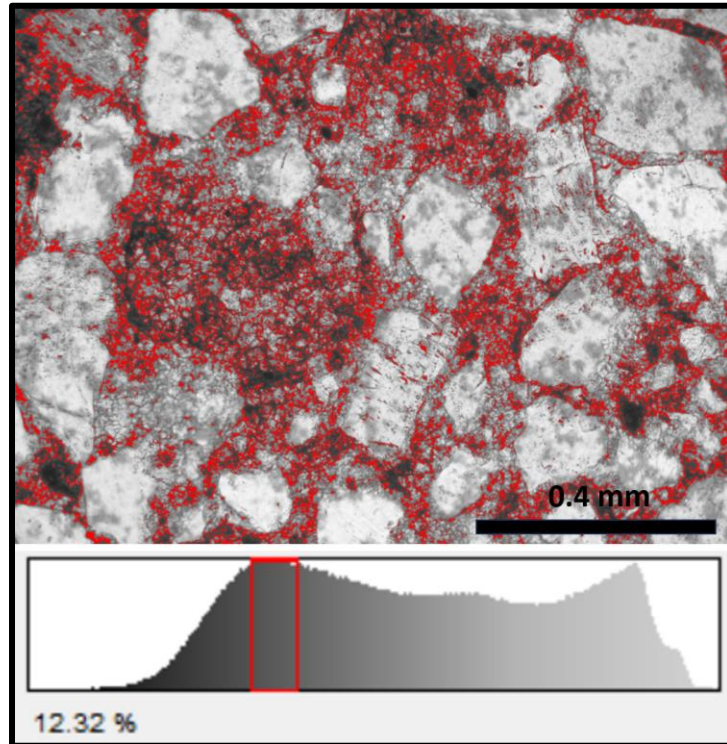


**Figure 23** Calculation of porosity for (S1) sample from Simre site by using imagej software.

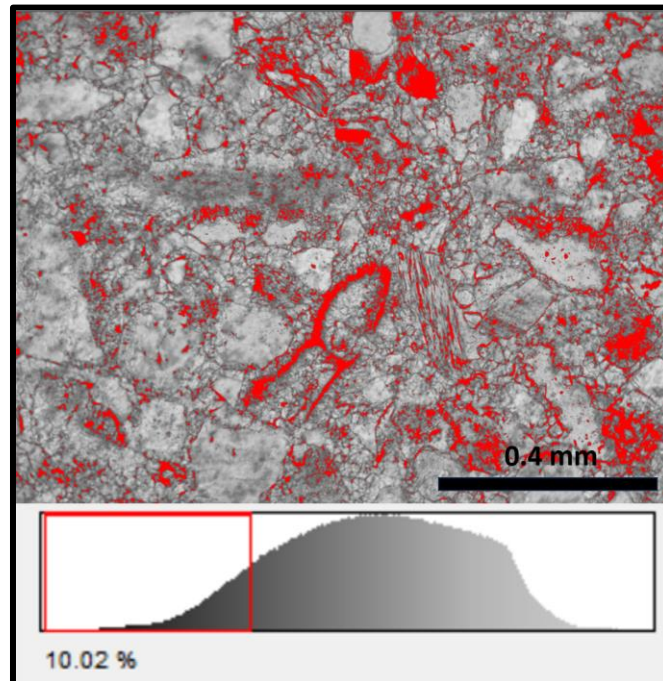


**Figure 24** Calculation of porosity for (DN1) sample from Dolní Nětčice site by using imagej software.

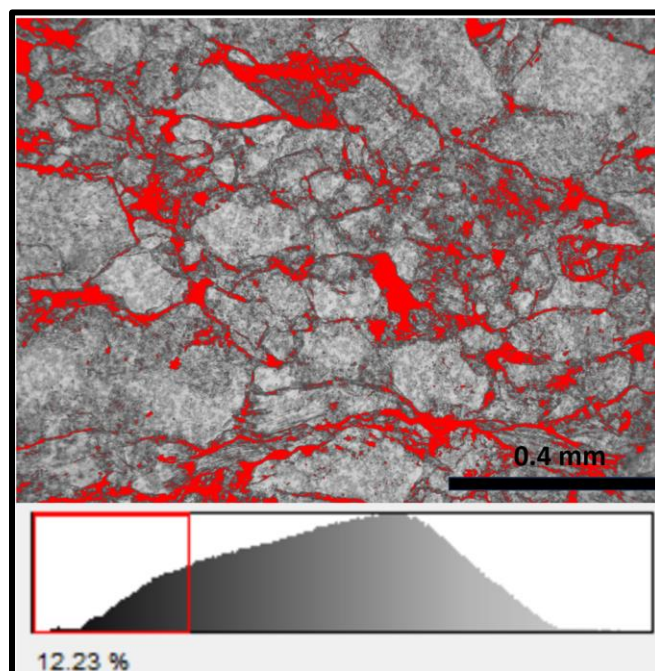


**Figure 25** Calculation of porosity for (DN2) sample from Dolní Nětčice site by using imagej software.

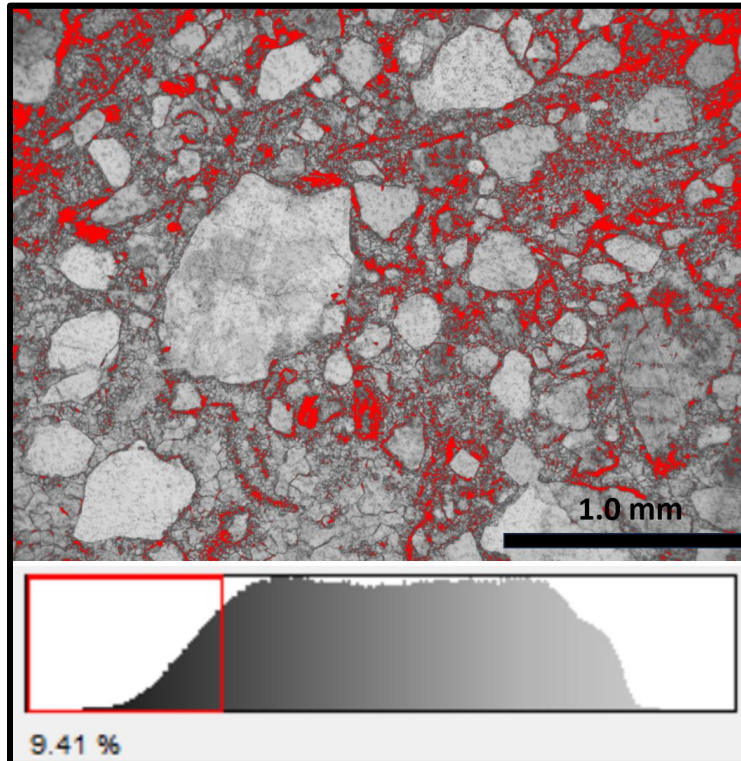


**Figure 26** Calculation of porosity for (DN3) sample from Dolní Nětčice site by using imagej software.

### 7.2 Evaluation of sensitivity of gamma-ray spectrometry to beds with different porosity

Gamma-ray spectrometry (GRS) is a valuable tool in evaluating the porosity of sedimentary rocks, as it measures the natural radioactivity of rocks primarily contributed by isotopes of Potassium (K), Uranium (U), and Thorium (Th). These measurements are useful indicators of lithology and can indirectly provide insights into the porosity of the rocks. Higher GRS values typically indicate higher clay and heavy mineral content, suggesting lower porosity due to finer grain size and reduced permeability. In the Figure 18, different rock types such as gravel, pebble sandstone, sandstone, and silty clay are displayed with their respective depths and GRS readings.

The lithologic column on the left side of the image represents various sedimentary layers from 0 cm to 560 cm in depth. Gravel, with likely high porosity, shows lower K, U, and Th values, as

these coarse sediments contain fewer clay minerals and heavy minerals. This is evident from the lower GRS values corresponding to gravel layers (Fig. 18).

Pebble sandstone, characterized by larger grain sizes and potentially higher porosity, also has relatively low GRS readings compared to finer sediments due to reduced clay content. This is depicted in the (Fig. 18) where pebble sandstone layers show lower K, U, and Th readings. Sandstone, which can vary in porosity, generally shows moderate GRS values depending on the degree of cementation and clay content. Sandstone layers display moderate K, U, and Th values, reflecting their variable porosity.

Silty clay, typically exhibiting low porosity due to the fine grain size, has higher GRS readings for K, U, and Th, reflecting the higher content of clay and heavy minerals. This is clearly illustrated in the (Fig. 18), where silty clay layers show higher GRS values. The Th/K ratio helps distinguish between different types of clay and feldspar, with a high ratio indicating an increase in heavy minerals or certain clays, suggesting lower porosity. The image demonstrates this with the Th/K ratio varying across different lithologies.

Additionally, the image includes a Standard Gamma-Ray (SGR) log on the far right, which integrates the GRS data into a single curve. This curve provides a comprehensive view of the natural gamma radiation, allowing for quick assessment of the overall radioactive content and thus the porosity and lithologic variations. The SGR log, depicted in black, shows fluctuations that correspond to changes in lithology, with peaks indicating higher radioactive content (and typically lower porosity) and troughs indicating lower radioactive content (and typically higher porosity).

## 6. Conclusion

The comprehensive analysis of sandstone samples from the Simre (S1) and Dolní Nětčice (DN1, DN2, DN3) sites reveals critical insights into the interplay between provenance, diagenetic factors, and the resulting porosity and permeability of the sandstones. Sandstones with higher porosity and permeability are associated with better sorting, subrounded grain shapes, and less extensive cementation and clay alteration. Conversely, sandstones with lower porosity and permeability are linked to poor sorting, subangular grain shapes, and significant cementation and clay presence. Gamma-ray spectrometry (GRS) is an invaluable tool for evaluating the porosity of sedimentary rocks by measuring natural radioactivity from Potassium (K), Uranium (U), and Thorium (Th). Higher GRS values typically indicate higher clay and heavy mineral content, suggesting lower porosity and reduced permeability. Gravel layers, with high porosity, exhibit low K, U, and Th values due to fewer clay and heavy minerals. Pebble sandstone, characterized by larger grain sizes and potentially higher porosity, also shows relatively low GRS readings due to reduced clay content. Sandstone layers display moderate K, U, and Th values, reflecting variable porosity depending on cementation and clay content. Silty clay, with low porosity, has higher GRS readings for K, U, and Th, indicating a higher content of clay and heavy minerals. The Th/K ratio helps distinguish between different clays and feldspar, with higher ratios indicating increased heavy minerals or certain clays, suggesting lower porosity. The Standard Gamma-Ray (SGR) log integrates GRS data into a single curve, providing a comprehensive view of natural gamma radiation; peaks in the SGR log indicate higher radioactive content and typically lower porosity, while troughs indicate lower radioactive content and typically higher porosity.

## 7. References

- Abu-Khamsin, S.A. (2004) *Basic Properties of Reservoir Rocks*. King Fahd University of Petroleum & Minerals, Dhahran, Saudi Arabia.
- Aldoury, M.M. (2010) 'A discussion about hydraulic permeability and permeability', *Petroleum Science and Technology*, 28(10), pp. 1740-1749.
- Arkalgud, R. and McDonald, A. (2020) 'Automated selection of inputs for log prediction models using domain transfer analysis (DTA) derivative', *Abu Dhabi International Petroleum Exhibition & Conference*. Available at: <https://doi.org/10.2118/203094-MS>
- Bakhtiari, H.A.V., Moosavi, A., Kazemzadeh, E., Goshtasbi, K., Esfahani, M.R. and Vali, J. (2011) 'The effect of rock types on pore volume compressibility of limestone and dolomite samples', *Geopersia*, 1(1), pp. 37-82.
- Bandara, K.M.A.S., Ranjith, P.G. and Rathnaweera, T.D. (2019) 'Improved understanding of proppant embedment behavior under reservoir conditions: a review study', *Powder Technology*, 352, pp. 170-192. Available at: <https://doi.org/10.1016/j.powtec.2019.04.033>
- Chen, Z. and Zhao, Y. (2022) 'A quasi-physical method for random packing of spherical particles', *Powder Technology*, 412, pp. 118002. Available at: <https://doi.org/10.1016/j.powtec.2022.118002>
- Dandekar, A.Y. (2013) *Petroleum Reservoir Rock and Fluid Properties*. 2nd edn. Boca Raton: CRC Press. Available at: <https://doi.org/10.1201/b15255>
- Francírek, M. and Nehyba, S. (2016) 'Evolution of the passive margin of the peripheral foreland basin: An example from the Lower Miocene Carpathian Foredeep (Czech Republic)', *Geologica Carpathica*, 67(1). Available at: <https://doi.org/10.1515/geoca-2016-0003>
- Folk, R.L. (1980) *Petrology of Sedimentary Rocks*. Austin, TX: Hemphill Publishing Co.
- Glover, P. (2001) *Formation Evaluation MSc Course Notes: Porosity*, Chapter 5: Porosity, pp. 43-53.
- Golonka, J. and Picha, F.J. (2006) 'Introduction', in: Golonka, J. and Picha, F.J. (eds.) *The Carpathians and their foreland: Geology and hydrocarbon resources*, AAPG Memoir 84, pp. 1-9.
- Huang, Q., Zhou, X. and Liu, B. (2023) 'Effect of realistic shape on grain crushing for rounded and angular granular materials', *Computers and Geotechnics*. Available at: <https://doi.org/10.1016/j.compgeo.2023.105659>

- McManus, J. (1988) 'Grain size determination and interpretation', in: Tucker, M.E. (ed.) *Techniques in Sedimentology*, pp. 63-85. Blackwell Scientific Publications.
- Milliken, K.L. (2003) 'Late diagenesis and mass transfer in sandstone shale sequences', in: *Treatise on Geochemistry*, 7, pp. 407.
- Ogolo, N.A., Akinboro, O.G., Inam, J.E., Akpokere, F.E. and Onyekonwu, M.O. (2015) 'Effect of grain size on porosity revisited', *SPE-178296-MS*. Available at: <https://doi.org/10.2118/178296-MS>
- Payton, R.L., Chiarella, D. and Kingdon, A. (2022) 'The influence of grain shape and size on the relationship between porosity and permeability in sandstone: a digital approach', *Scientific Reports*, 12, 7531. Available at: <https://doi.org/10.1038/s41598-022-11365-8>
- Rutter, E.H. and Glover, C.T. (2012) 'The deformation of porous sandstones; are Byerlee friction and the critical state line equivalent?', *Journal of Structural Geology*, 44, pp. 129-140. Available at: <https://doi.org/10.1016/j.jsg.2012.08.014>
- Sanders, C., Huisman, R., van Wees, J.D. and Andriessen, P. (2002) 'The Neogene history of the Transylvanian Basin in relation to its surrounding mountains', *Tectonophysics*, 354(1-4), pp. 1-25. Available at: [https://doi.org/10.1016/S0040-1951\(02\)00252-1](https://doi.org/10.1016/S0040-1951(02)00252-1)
- Santschi, P., Höhener, P., Benoit, G. and Buchholtz-ten Brink, M. (1990) 'Chemical processes at the sediment-water interface', *Marine Chemistry*, 30, pp. 269-315.
- Šimíček, D. and Bábek, O. (2015) 'Assessing provenance of Upper Cretaceous siliciclastics using spectral  $\gamma$ -ray record', *Geocarta International*, 30(2), pp. 150-165. Available at: <https://doi.org/10.1515/geoca-2015-0028>
- Stanley-Wood, N.G. and Lines, R.W. (eds.) (1992) *Particle size analysis*. The Royal Society of Chemistry, Cambridge. pp. xx + 538. ISBN 0 85186 487 2.
- Wentworth, C.K. (1922) 'A scale of grade and class terms for clastic sediments', *The Journal of Geology*, 30(5), pp. 377-392.